Mathematical modelling of a reciprocating compressor with coolant injection and valve control

By

Abraham Carel Plekker

Dissertation submitted in the fulfilment of the requirements for the degree

MASTER OF ENGINEERING

IN

MECHANICAL ENGINEERING

In the

Department of Mechanical and Mechatronics Engineering

Faculty of Engineering, Built Environment and Information Technology

at the Central University of Technology, Free State.

Bloemfontein 2024

Supervisor: **Dr. G.G. Jacobs, Ph.D.**

Central University of Technology, Free State

Co-supervisor: **Prof. A. Romagnoli, Ph.D.**

Nanyang Technological University, Singapore

Abstract

Compressed air is used throughout industry in various forms, ranging from small pneumatic tools to long pipelines at mines, and it accounts for 9%–10% of total energy consumption. Many energy providers utilise fossil fuels for electricity production, which has prompted the need to invest in renewable energy solutions. The cost of a compressed air system depends on multiple components, the largest being energy cost, which accounts for 75%–80% of the total life-cycle cost of the system. Thus, with increased efficiency, the cost and energy consumption of compressed air will decrease.

The aim of this research is to further investigate the effects of timed coolant injection in a reciprocating compressor to create a quasi-isobaric process followed by a quasi-isothermal process with the aim to increase compressor efficiency. A mathematical model and numerical simulation, utilising the first law of thermodynamics, was created to simulate the effects of timed coolant injection at the commencement of the compression stroke.

The mathematical model and numerical simulation were validated against experimental results and exhibited being in good agreement. The application of the mathematical model beyond its tested operating range was also presented.

Acknowledgements

First and foremost, I would like to thank God. He gave me this opportunity and provided me with the strength to persevere through all the challenging moments of completing this dissertation.

I would like to express my deepest appreciation to Dr Gys Jacobs, without whom this research study would not have been possible. Not only was academic knowledge imparted but also stories shared, life lessons learned, professional guidance given, and endless jokes made, culminating in a life-long relationship.

A special thank you to Prof. Alessandro Romagnoli at Nanyang Technological University, Singapore, who initiated this study through his collaboration with Central University of Technology, Free State.

I would like to thank the Product Development Technology Station for supporting my part-time academic pursuit. Dr Michelle Erasmus for her unyielding positivity and assistance with the Runge-Kutta method. Dr Jacques Combrinck and Dr Kobus van der Walt for their support, both personally and administratively. Dr Maina Maringa for his timely encouragement, given unintentionally, multiple times in the parking garage of the Engineering Faculty.

I would also like to extend my deepest gratitude to my parents, Pierre and Sandra, who supported me throughout and whose hard work funded this study.

And, lastly, my dearest wife Azahndri, thank you for your immense support, understanding, and patience. Your encouragement and empathy carried me across the line.

Dedication:

To my family.

Central University of Technology, Free State

Contents

LIST OF TABLES

LIST OF FIGURES

NOMENCLATURE

Roman letters

Symbol	Description	Unit
A	Area	m^2
A_{dv}	Area of discharge valve	m^2
A_{eff}	Effective valve area	m^2
A_o	Valve opening area	m^2
A_p	Area of valve port	m^2
A_{sv}	Area of suction valve	m^2
c	Damping coefficient	Ns/m
C_D	Coefficient of discharge for orifice flow	-
CF_w	Cylinder wall heat transfer calibration factor	-
C_f	Spring force coefficient	-
C_p	Specific heat capacity at constant pressure	J/kg.K
C_v	Specific heat capacity at constant volume	J/kg.K
D	Diameter	m
D_e	Characteristic diameter	m
F_{act}	Spring actuating force	N
h_w	Coefficient of wall heat transfer	
i	Program step	
k	Thermal conductivity	W/m.K
L	Compressibility factor	-
m	Mass	kg
$\dot{m}_{coolant}$	Coolant mass flow	kg/s
$\dot{m}_{DRYRUN}$	Compressor mass flow without coolant injection	kg/s
N	Compressor speed	rev/min
n	Polytropic index	-
Nu	Nusselt number	-
P	Pressure	Pa
Pr	Prandtl number	-
Q	Heat energy	J
q	Heat transfer	W.m.K
R	Gas constant	J/kg.K
S	Stroke length	m
T	Temperature	K
t	Time	s
U	Internal energy	J
V	Volume	m^3
v	Velocity	m/s
v_{piston}	Mean piston velocity	m/s
W	Work	J
x	Displacement	m

Greek letters

Symbol	Description	Unit
B	Velocity of jet coefficient	
Φ	Adiabatic mixing effectiveness factor	-
γ	Specific heat ratio	-
ϵ	Compressor efficiency	-
κ	Spring stiffness	N/m
μ	Working fluid kinematic viscosity	m^2/s
ξ	Valve entrance friction coefficient	-
π	Pi	
ρ	Density	kg/m
ω	Crank angular velocity	rad/s

Subscripts

Symbol	Description
cle	Clearance
cyl	Cylinder
c	Coolant
d	Discharge
d_v	Discharge valve
e	Equivalent
g	Gas
i	Index variable
i	Initial
i	Instantaneous
o	Open
pre	Preload
s	Suction
str	Stroke
sv	Suction valve
w	Cylinder wall

Abbreviations

CAES	Compressed Air Energy Storage
PHS	Pumped Hydro-electric Schemes
CES	Cryogenic Energy Storage
FS	Full Scale
LAES	Liquid Air Energy Storage
GHG	Greenhouse Gas
ORC	Organic Rankine Cycle

TDC	Top Dead Centre
CFD	Computational Fluid Dynamics
ISO	International Organization for Standardization
ASHRAE	The American Society of Heating, Refrigerating and Air-Conditioning Engineers
AHRI	Air-Conditioning, Heating and Refrigeration Institute
ODE	ordinary differential equations
EES	Engineering Equation Solver
ERD	Euclidean Relative Difference
EPC	Euclidean Projection Coefficient
SC	Secant Cosine

Chapter 1: Introduction

1.1 Background

1.1.1 Application of compressors

Compressors are used to deliver a quantity of fluid, either a gas or vapour, while increasing its pressure [1], [2]. The applications of compressors vary, with the fluid discharge mass flow rate, discharge pressure, and compression mode being the determining factors [1], [2].

These factors contribute to the classification of compressors into two broad groups: intermittent flow and continuous flow [1], [2]. Based on the performance of various compressor types, the reciprocating and rotary-type compressors are distinctly intermittent with low mass flow rates and high discharge pressures, while radial-flow, mixed-flow, and axial-flow compressors discharge a continuous, high mass flow, low pressure stream of fluid [1], [2].

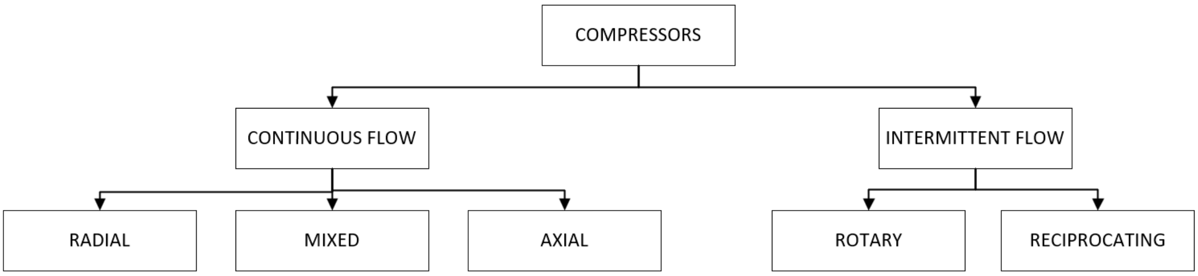

Figure 1: Compressor classification (adapted from [2])

Reciprocating compressors have a series of applications ranging from household to industrial use. Standard reciprocating compressor pressures can range from 0.6 bar to 20 bar [3]. An increase in discharge pressure increases the temperature of the working fluid, decreasing overall efficiency. It is common practice to make use of multistage reciprocating compressors with intercooling between each stage for discharge pressures above 5.5 bar [3].

Compressed Air Energy Storage (CAES) works similar to Pumped Hydro-electric Schemes (PHS) [4]. Both CAES and PHS utilise excess (off-peak) power to store energy which can be used at times of peak power demand. The difference between CAES and PHS is the working fluid, which, in the case of CAES, is air.

CAES compresses ambient air to a high pressure and stores it in a large underground cavity. The pressure inside the cavity can range from 45 bar to 72 bar [4]. The only two operational CAES plants in the world utilise excavated salt deposits as storage cavities. These plants are located in Huntorf, Germany and McIntosh, Alabama in the United States [5], [6]. When electricity consumption is high, the compressed air is mixed with natural gas, ignited, and expanded through a turbine which generates electricity. The electricity is transferred to the electric grid supplying homes and industry [5].

Another method of compressed air storage is Cryogenic Energy Storage (CES). The CES process consists of air which is compressed, cooled, and expanded until liquefied and subsequently stored in insulated storage containers at atmospheric pressure [7].

Several cycles are used to achieve the liquefaction of air, namely: the Joule-Thomson, Hampson-Linde, Reverse Brayton, Kapitza, and Claude cycles [8]. The Hampson-Linde cycle, which comprises of a compressor, cooler, heat exchanger, expander, and storage tank, is commonly used for the manufacturing of liquid air [9], [10]. The Claude cycle (and variants thereof) is implemented by Highview Power in the only utility-scale Liquid Air Energy Storage (LAES) facility [11], [12]. The Joule-Thomson effect, where real gases experience a decrease in temperature when throttled, is utilised during the Hampson-Linde and Claude cycles [9], [13].

CES and CAES systems have comparable round-trip efficiency [9]. An overall increase in compressor efficiency would have a direct positive impact on the round-trip efficiency of CES and CAES systems [14], [15].

1.1.2 Energy consumption of compressors and compressed air systems

Compressed air is used throughout various industries, with uses ranging from small pneumatic tools in the manufacturing sector to long pipelines at mines. The wide use of compressed air equates to between 9% and 10% of total electricity consumption in industry worldwide [16]. The South African mining and industrial sectors consume a combined 67% of the total electricity generated by Eskom on an annual basis [17].

The total cost of a compressed air system, when calculated over its lifetime, depends on a few key aspects: energy cost, capital/investment cost, and maintenance cost. The energy or electricity use of a compressed air system constitutes the largest part of the cost, ranging between 75% to 80% of the overall lifetime cost [2] – [5].

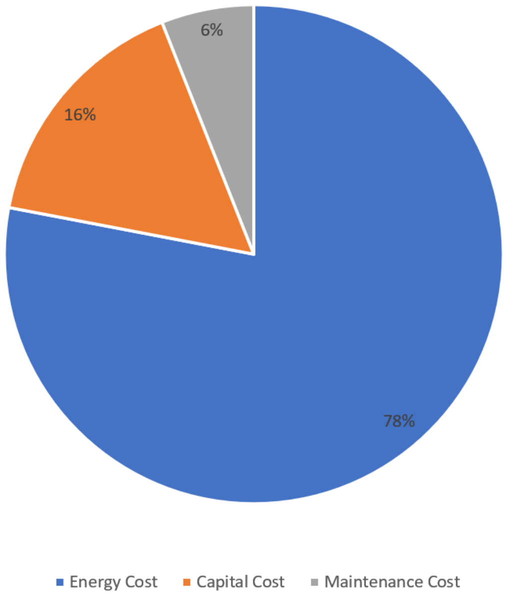

Figure 2: Total cost of compression system, adapted from Saidur et al. [16]

Compressed air is an inefficient form of energy, with only up to 19% of the energy consumed converted into usable compressed air [16], [19], [20]. Thermal energy that is lost to the surroundings constitutes the largest part of the total energy loss of a compressed air system [20]. The overall efficiency of a compressor is derived from the sum of the electrical, mechanical, and thermal efficiency, with the latter also the least efficient at between 80% and

83% [21]. An increase in compressor thermal efficiency would thus yield and increase the overall compressor efficiency and compressed air system efficiency.

1.2 Motivation for the study

The effects of climate change are felt globally. The Intergovernmental Panel on Climate Change and Nongovernmental International Panel on Climate Change agree that the main cause of climate change is the increase of anthropogenic Greenhouse gas (GHG) concentrations in the atmosphere [22].

Since the burning of fossil fuels is the main cause of increased concentrations of GHG in the atmosphere, one solution to counter this is to replace fossil fuels with renewable energy sources. Another method of decreasing GHG concentrations is the increased efficiency of current energy-consuming machines and systems.

1.3 Purpose of the study

The aim of this research is to develop and validate a mathematical model, based on the first law of thermodynamics, for a reciprocating compressor subjected to coolant injection and valve control. Such a model will support the development of reciprocating compressors with improved efficiency.

1.4 Delimitations

Throughout this research the working fluid is assumed to be an ideal gas.

The following will be excluded from this study:

- Effect of coolant evaporation during compression is ignored;
- The analysis of geometric features such as cylinder diameter and stroke will not be conducted;
- A comprehensive CAES process model will not be created;
- Design recommendations or improvements to the experimental compressor will not be made; and
- Additional experimental work was not possible since the validation of the mathematical model and numerical simulation is based on the results published in 2024 of a compressor tested at North-West University [53].

1.5 Dissertation layout

Chapter 2 presents a literature review focusing on research pertaining to increasing compressor efficiency through coolant injection. Chapter 3 presents a mathematical model, which will be used to simulate a reciprocating compressor with timed coolant injection by applying the first law of thermodynamics. The validation of, and subsequent results from the mathematical model and simulation, is summarised in Chapters 4 and 5. Finally, Chapter 6 provides a summary and conclusion of the research conducted.

Chapter 2: Literature review

2.1 Introduction

This chapter reviews prior research conducted on the improvement of compressor efficiency through various cooling methods, with emphasis on in-cylinder coolant injection. Mathematical modelling of compressors with coolant injection is also discussed.

2.2 Increasing compressor efficiency

The first law of thermodynamics states that the change in internal energy (ΔU) is equal to the change in the work done (W) on the system and the heat energy (Q) which is generated or rejected, see equation (1) [23]. For a compressor, these energies represent the transfer of mass from a low pressure to a high pressure, the heat generated, and the work done per cycle.

$$\Delta U = W - Q \tag{1}$$

It is thus evident that the efficiency of a compressor is dependent on, but not limited to, the amount of energy lost to its surroundings due to heat generation [24].

Compressor efficiency can be maximised if the working cycle is internally reversible; that is, the working fluid and its surroundings are in a constant state of equilibrium [1], [24]. This can be achieved if the compression and expansion processes occur at a slow rate, which enables the working fluid to either absorb or dissipate heat to achieve energy equilibrium at each time step. In practice, an internal reversible process cannot be achieved within reasonably practical and economic limits.

The equilibrium state of an internally reversible compressor can be imitated through various means to achieve a quasi-equilibrium state [25]. This quasi-equilibrium state is achieved through the effective cooling of the working fluid during compression.

The effect of cooling on the compression process can be examined through the comparison of different compression processes (*cf*. Figure 3). These polytropic processes, depending on the polytropic index n, influence the amount of work done on the system as shown on the Temperature-Entropy (T-S) and Pressure-Volume (P-V) diagrams in Figure 3 and Figure 4.

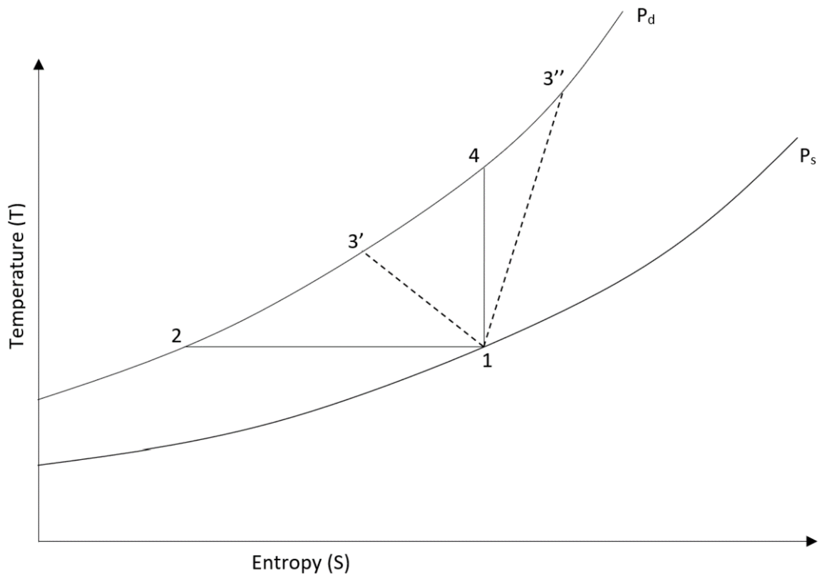

Figure 3: Temperature-Entropy (T-S) diagram

Figure 4 shows polytropic processes on a Temperature-Entropy (T-S) diagram.

The compression process between points 1 and 2 shows an ideal isothermal (constant temperature) process, where $n = 1$. Between points 1 and 4, an ideal isentropic (constant entropy) process, where $n = \gamma$, is shown. This is also known as an adiabatic process. Between points 1 and 3' and points 1 and 3'', two polytropic processes are shown, where $1 < n < \gamma$ and $n > \gamma$ respectively.

The saving in work between the processes can be displayed on a P-V diagram (*cf*. Figure 4). The amount of work required during the process is shown by means of the grey shaded area (1-4-5-6) between the suction (P_1) and discharge (P_2) pressures. The compression process between points 1 and 2 shows an ideal isentropic process, between points 1 and 4 an ideal isothermal process, and between points 1 and 3 a polytropic process.

An isentropic process requires the complete insulation of the system to ensure that no heat is rejected to the atmosphere. This process is less likely to be experimentally or industrially achievable, as no system can be fully insulated [23], [24].

In most cases, the heat rejected by the compressor is regarded as waste heat and simply rejected to the atmosphere. However, this waste heat can be recovered using an Organic Rankine Cycle (ORC) or a Kalina cycle [26], [27]. These cycles harvest low grade heat, between 30°C and 200°C, with a heat exchanger which heats the organic working fluid and drives a turbine or expander to generate electricity. Murgia et al. [27] suggest the use of ORCs to generate electricity for use by the compressor, thus resulting in an overall decrease in entropy, or to supply the local electrical grid [28].

Shuaihui et al. [29] proposed the addition of an externally mounted cooling chamber to a scroll compressor, which has cooling water flowing through channels that, in turn, cool both the fixed scroll bed and the fixed scroll cover. The addition of this cooling chamber resulted in a 7.4% increase in isentropic efficiency [29].

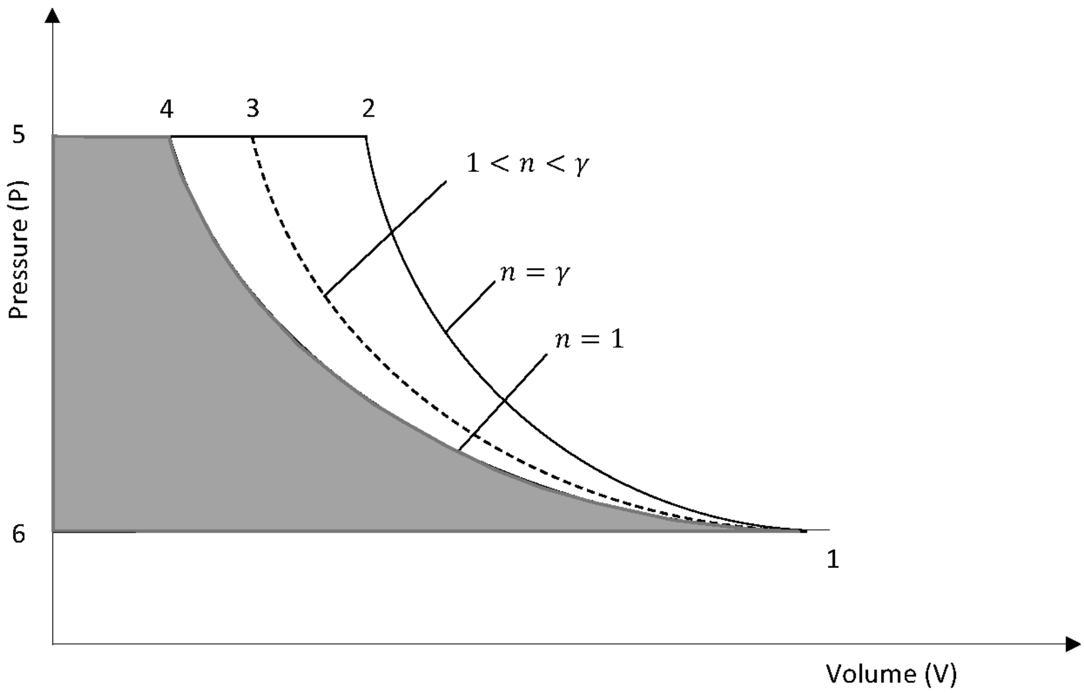

Figure 4: Pressure-Volume diagram representing isentropic and isothermal compression, adapted from X.Wang et al. [30]

If no effort is made to cool down the compressor externally, either by means of a fan blowing over the casing, adding a cooling jacket around the casing, or altering the compression process in any way, the above-mentioned methods of recovering waste heat can be utilised. However, utilising other compression processes can reveal other, more significant, thermal efficiency improvement options.

Quasi-isothermal compression is achievable if the heat of compression is removed continuously during the compression process $1-2$ (*cf.* Figure 3). This is also the process which requires the least amount of work and is thus the most desired compression process.

Wang et al. [30] proposed a combination of isothermal and isentropic compression for the cooling of a scroll compressor for air-conditioning applications. The author predicted an efficiency increase of 16% for said compressor. While Wang et al. [30] mentioned refrigerant injection as a possible method of cooling the compressor, the author decided to model the compressor on a theoretical basis only, with no mention of practically achieving the desired processes. Research was conducted on in-cylinder liquid injection (A.K. Dutta et al. [31], B. Wang et al. [32]), vapour injection (H. Sun et al. [33]), and liquid flooding (I.H. Bell [34]) of scroll compressors, which shows efficiency increases due to quasi-isothermal compression being achieved.

Similar research was conducted for other types of compressors, which include screw compressors (K. Hammerl et al. [35], M. de Paepe et al. [36]) and axial flow compressors (D.P. Georgiou et al. [37]).

Quasi-isothermal compression in reciprocating compressors can be accomplished with the use of multistage compressors with intercooling between stages. Multistage compressors have multiple cylinders with which to compress the working fluid. An intercooler is added between these stages to cool the working fluid after compression, reducing the amount of work needed during the next compression stage [38], [39]. It should be noted that perfect intercooling between each stage is the theoretical ideal for multistage compression with interstage cooling [40].

Multistage compressors with intercooling have an increased parts count and complexity compared to single-stage compressors, which adds to the initial capital cost of such a multistage compressor but reduces the energy consumption costs over the life of the compressor. The limitations of achieving quasi-isothermal compression with the use of external components and processes have caused researchers to investigate methods of achieving quasi-isothermal compression with in-cylinder heat exchange processes [41].

In-cylinder quasi-isothermal compression can be divided into two main groups, namely: Dry compression mechanisms (with indirect heat transfer) and wet cooling compression processes (with direct contact heat transfer between working fluid and coolant).

During dry quasi-isothermal reciprocating compression processes, most of the compression work is done on the working fluid as the piston reaches its Top Dead Centre (TDC). This is when the most heat is generated – while the contact area between the cylinder walls and the working fluid is smallest [41].

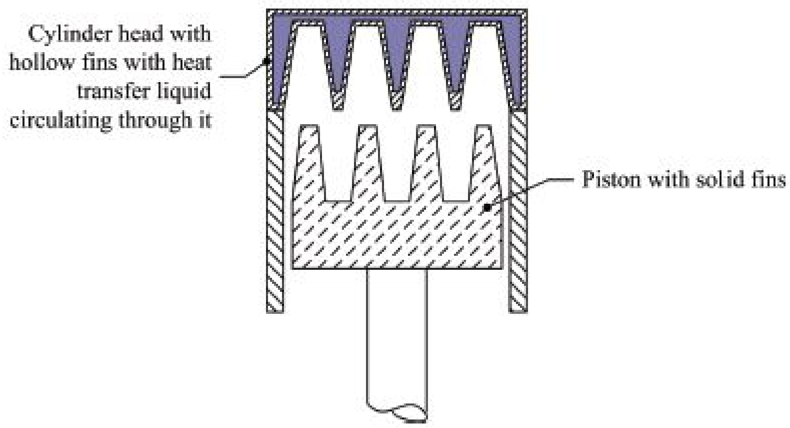

Figure 5: Dry expansion finned piston, adapted from [38]

- Dry compression mechanisms:

Heidari and Rufer [42] put forth a novel design which utilises internal fins constructed as annular intersecting fins, which increase the contact area during compression drastically [42]. The finned piston showed an increase in exergetic efficiency of 11.7% over that of a standard piston [42].

Research conducted by Knowlen et al. [43] for the quasi-isothermal expansion of liquid nitrogen, for use as an automotive engine, utilises a similar design to that implemented by Heidari and Rufer [42] (*cf*. Figure 5). Applying the finned piston, Knowlen et al. claim an isothermal efficiency of 85%. The expander configuration with finned piston proposed by Knowlen et al. can be implemented as a compressor.

- Wet compression cooling processes:

Most research conducted on quasi-isothermal compression entails introducing liquid coolant into the compression chamber. The coolant can either be mixed with the air prior to the commencement of the suction stroke or directly injected into the cylinder during compression. This results in direct heat exchange between the compressed gas and coolant, i.e., a directly cooled compression process.

Van de Ven and Li [44] proposed the use of a liquid piston utilising a column of liquid inside a fixed volume/cylinder, which is used for gas compression and expansion [44]. The conceptual design of the liquid piston compressor does not differ from the conventional reciprocating compressor designs currently in use. A column of liquid rests on a flat-faced piston inside the cylinder, which negates the need for piston seal rings and eliminates air leakage between the cylinder wall and piston.

Van de Ven and Li [44] showed a 19% decrease in work required during compression, resulting in an increase of compression efficiency of up to 83%. This is largely due to the reduction in mechanical friction, from the elimination of the piston seal rings, and the nonconformity of the liquid column shape, which increases the heat transfer area between the column and the working fluid.

Qin et al. [45] investigated the cooling effect of coolant injection for a liquid piston. This research showed an increase in compression efficiency of up to 27%, resulting in an overall efficiency of 98% when the mass of water injected is five times the mass of dry air in the cylinder.

Research conducted by Shcherba et al. [46] investigated the optimal operating speed of the liquid piston to reach an isothermal compression process. A two-stage reciprocating compressor was used with the first stage being a noncooled compression process and the second stage being a liquid piston compression process. Shcherba et al. [46] showed that a liquid piston average speed of 3 m/s is required to increase the probability of achieving isothermal compression. An indicator efficiency increase of up to 20% was achieved.

2.2.1 Reciprocating compressors with coolant injection

Direct cooled compression processes also include a standard reciprocating compressor equipped with coolant injection. Coolant in the form of oil, refrigerant, water, etc. is injected directly into the cylinder during the compression stroke [47], [48]. The injected coolant mixes with the working fluid and absorbs the heat generated during compression, resulting in a quasi-isothermal process [25], [47].

Kremer et al. [49], [50] created two mathematical models simulating the injection of oil as a coolant for a reciprocating refrigerant compressor using ammonia and R-134a respectively. The ammonia refrigerant compressor showed a reduction in energy use of up to 4.2%, but the author noted that this reduction in energy use cannot be achieved in practice without the use of an external oil cooling source [49]. The R-134a refrigerant compressor showed an increase in cooling capacity, but this positive was offset by an increase in power consumption [50].

Research pertaining to direct water coolant injection for quasi-isothermal compression was performed by Coney et al. [25] which highlighted the factors influencing heat transfer with 3D Computational Fluid Dynamic (CFD) simulations. Coney et al. [25] stressed that there is limited time to inject water into the cylinder, but two approaches can be taken, namely early and late injection. Early injection, which occurs during the suction stroke, has the benefit of a high droplet dispersion and penetration rate; however, this results in a low droplet velocity during the compression stroke, lowering the heat transfer rate at the point of high heat generation. Late injection, which occurs during the compression stroke, is the desired injection time, with heat generation highest, but with a higher working fluid density, which results in poor droplet penetration to the centre of the cylinder. This problem was overcome by increasing the size of the water droplets injected into the cylinder during the compression stroke.

Malmgren et al. [51] subsequently created and validated a 1-D dynamic mathematical model to simulate the compressor tested by Coney et al. [25].

Jacobs and Liebenberg [52] have shown that even higher compressor efficiencies can be obtained. The process proposed by Jacobs and Liebenberg [52] involved isobaric cooling at the commencement of the compression stroke, through suction valve control, followed by isothermal compression. The process is depicted on T-S and P-V diagrams in Figure 6.

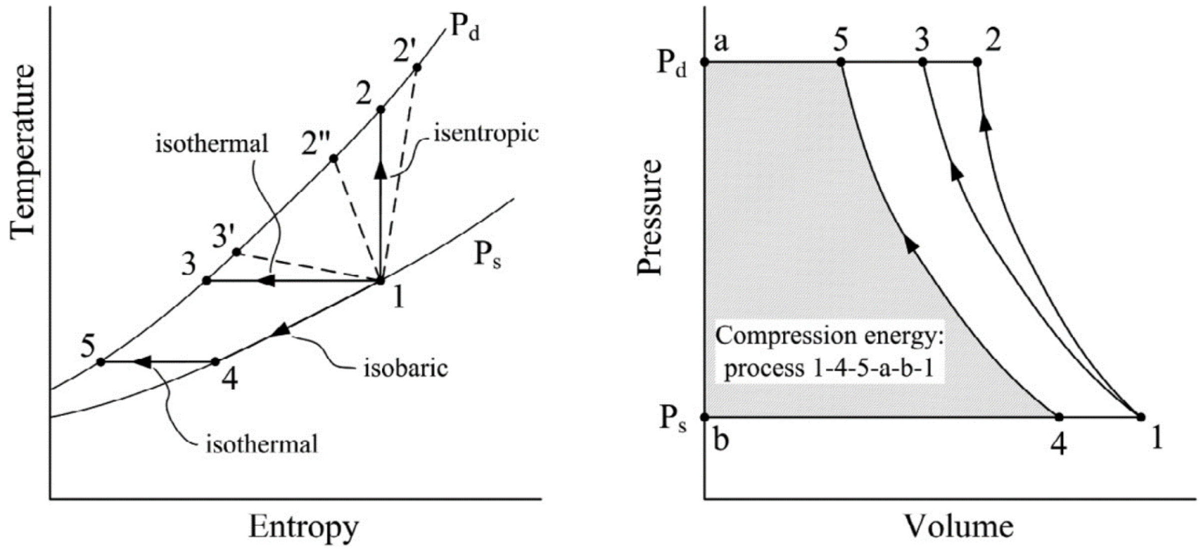

Figure 6: Pressure-Volume and Temperature-Entropy diagrams showing the energy saving when isobaric compression is followed by isothermal compression [52]

The isobaric cooling process (*viz.* process 1–4 in Figure 6) is achieved by a sudden and significant cooling effort, achieved with water coolant injection, at the commencement of the compression stroke. The authors found that the increase in density of the working fluid, due to the coolant injection, created a quasi-isobaric compression process, which resulted in a decrease in work done during the initiation of the compression stroke.

The quasi-isobaric conditions can only be achieved if the suction valve is kept in a closed position during coolant injection. The authors utilised a camshaft to control the suction valve and actuate the coolant injection valves.

Quasi-isothermal compression was achieved by injecting sufficient coolant into the cylinder during the compression stroke. The quasi-isobaric compression process showed a 6% increase in isothermal efficiency compared to a quasi-isothermal process. The quasi-isobaric compression process coupled with a quasi-isothermal compression process led to a further 3% increase in isothermal efficiency, equating to 89% isothermal efficiency [52].

Jacobs and Liebenberg created a mathematical model to describe this novel compression process [52], [53]. This mathematical model was based on describing the compression and expansion processes as polytropic processes. The authors modelled continuous coolant injection, where $1 < n < \gamma$, as well as timed coolant injection, where $0 \leq n_{cool} \leq \gamma$. The mathematical model was validated against experimental results where a single cylinder, single acting compressor was used.

The authors noted that the limitation to the mathematical model is the polytropic index which should be determined through experimentation. Thus, to better investigate the effect of timed cooling and determine the amount of heat removed during isobaric cooling, it was proposed that a similar model based on the first law of thermodynamics be created.

2.3 Cylinder wall convective heat transfer

To determine the amount of heat removed during isobaric cooling, the loss of heat through the cylinder walls should be accounted for with a heat transfer coefficient. Various heat transfer correlations have been developed for both compressors and internal combustion engines.

Annand [54] and Woschni et al. [55] both developed convective heat transfer correlations to calculate the instantaneous heat transfer rate to the cylinder wall of an internal combustion engine by calculating the Nusselt number. Annand [54] utilises both the Reynolds and Prandtl number, while Woschni et al. [55] uses only the Reynolds number.

Subsequently, Adair et al. [56] developed a convective heat transfer correlation specifically for reciprocating compressors. Comparisons were made between various heat transfer correlations, and it was concluded that a variable characteristic cylinder diameter should be introduced; but, more importantly, the characteristic velocity, in contrast to the previously used mean velocity, should also be introduced.

This correlation by Adair et al. [56] has been widely used (see Table 2) and is expressed as:

$$Nu = 0{,}053{R_e}^{0{,}8}Pr^{0{,}6} \tag{2}$$

where Re is the Reynolds number and calculated with the following equation:

$$R_e = \frac{v_e D_e}{\mu} \tag{3}$$

where μ is the kinematic viscosity of the working fluid, v_e is the characteristic gas velocity and D_e is the characteristic cylinder diameter. v_e and D_e is calculated with:

$$v_e = 2\omega[1.04 + \cos(2\alpha)], \qquad for\ \frac{3}{2}\pi < \alpha < \frac{1}{2}\pi$$
$$v_e = \omega[1.04 + \cos(2\alpha)], \qquad for\ \frac{1}{2}\pi < \alpha < \frac{3}{2}\pi \tag{4}$$

where ω is the angular velocity of the crankshaft, and

$$D_e = \frac{6 \times Volume}{Area} = \frac{6 \times \left(\pi \times \frac{D}{2}\right)^2 \times S(t)}{\pi \times D \times S(t) + 2\pi \times \left(\pi \times \frac{D}{2}\right)^2} \tag{5}$$

where D is the cylinder diameter and $S(t)$ is the stroke length, as a function of time.

In 1994, Fagotti et al. [57] compared the convective heat transfer correlation of Adair et al. [56] with that of others and found that it does not fit the instantaneous measured experimental data well. The authors found that the correlation of Annand et al. [54] best fit the experimental data. In 1998, Fagotti et al. [58] proposed a new correlation for heat transfer between the gas and the cylinder wall. The authors proposed new constants for determining the Nusselt number, which is only applicable to the compressor model used to determine the constants.

In 2012, Disconzi et al. [59] proposed heat transfer correlations for the suction, discharge, expansion, and compression processes. The correlation is similar to that of Adair et al. (see Eq. (2)), with the Nusselt number calculated by equating the Reynolds and Prandl numbers but with different constants for each process. Table 1 below shows the constants of each process.

Table 1: Convective heat transfer correlations

Author	**Year**	**Correlation**	**Process**	**Reynolds number equation**	**Constants**
Annand	1963	$Nu = aR_e{}^b$		$R_e = \frac{vD}{\mu}$	0,35 $\leq a \leq$ 0,8; b=0,7
Woschni	1967	$Nu = aR_e{}^b$		$R_e = \frac{vD}{\mu}$	a=0,035; b=0,8
Adair	1972	$Nu = aR_e{}^b Pr^c$		$R_e = \frac{v_e D_e}{\mu}$	a=0,053; b=0,8; c=0,6
Fagotti	1998	$Nu = aR_e{}^b + c \times L \frac{T_w}{T_g - T_w}$		$R_e = \frac{v_e D_e}{\mu}$	a=0,28; b=0,65; c=0,25
Disconzi	2012	$Nu = aR_e{}^b Pr^c$	Suction Expansion Compression Discharge	$R_e = \frac{vD}{\mu}$	a=0,08; b=0,9; c=0,6 a=0,12; b=0,8; c=0,6 a=0,08; b=0,8; c=0,6 a=0,08; b=0,8; c=0,6

where L is the compressibility factor.

Tuhovcák et al. [60] compared the correlations of Annand, Adair, Disconzi, Aigner, and Woschni to determine the effect of the heat transfer on compressor efficiency. The authors found that each correlation predicts a different amount of heat transfer due to the differing methods of calculating the Reynolds number as well as the characteristic velocity used. Tuhovcák et al. [61] went further in 2016 and compared the heat transfer correlations of Annand, Adair, Disconzi, and Woschni but separated the heat transfer area inside the cylinder into the head, piston, and wall. The authors found that simulating only the three surface areas, without consideration for the different processes, negatively affected the accuracy of the simulation.

Table 2 shows the heat transfer correlations used by different authors simulating reciprocating compressors. Adair is shown to be the popular correlation with recent studies continuing its use into the 2010s.

Table 2: Authors utilising convective heat transfer correlations

Author	**Year**	**Correlation used**		
		Annand	**Woschni**	**Adair**
Prakash	1974			X
Brok	1980			X
Todescat	1992	X		X
Armaghani	2012		X	
Disconzi	2012			X
Heidari	2014			X

2.4 Compressor valve dynamics modelling

Reciprocating compressors commonly use automatic, self-acting valves that are activated by a change in pressure across the valve face [1]. Reed valves (*cf.* Figure 7) are commonly used in typical smaller household compressors on both the suction and discharge side [62]. Various versions of reed valves with different degrees of complexity are used, while large industrial compressors and the discharge side of some compressors incorporate more complex designs (*cf.* Figure 8) [62], [63].

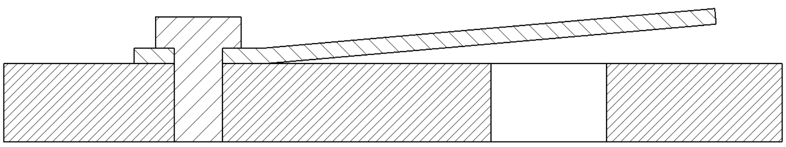

Figure 7: Schematic of simple reed valve without dampers

The more complex valve designs include a sealing element, highlighted in green and blue in Figure 8, consisting of either a plate, poppet, or ring manufactured from a thermoplastic [63]. These sealing elements' movement is damped by either a spring or nonsealing damping plate [63], [64].

(a) (b) (c)

Figure 8: (a) Plate valve, (b) Poppet valve, and (c) Ring valve, from [63]

Böswirth published various research articles and a book on the subject of compressor valves from 1980 to 2001, which built on the pioneering works of Costagliola [63] from 1950. In 2002, Bukac [62] presented a summary of the modelling of valve dynamics, while, in 2005, Habing [65] presented a thesis where a modern CFD approach was used to study valve dynamics and analyse historical semi-empirical coefficients. Ninković et al. [63] presented a summary paper on the research up to 2013 and concluded that valve modelling remains a research subject.

Valves are typically modelled as spring-mass-damper systems with a single degree of freedom [53], [63], [66], [67], [68] with the following equation:

$$m_{valve}\frac{d^2x}{dt^2} + c\frac{dx}{dt} + \kappa\left(x + x_{pre}\right) = F_{act}, for\ 0 < x < x_{max} \tag{6}$$

where m_{valve} is the valve plate mass, x is valve displacement, κ is the spring stiffness, c is the damping coefficient, and F_{act} is the spring actuating force. If a valve limiter is present, the valve will bounce when the limiter is reached. Habing et al. [66] modelled this bounce with a restitution coefficient:

$$\frac{dx}{dt}(t_+) = -e_{res}\frac{dx}{dt}(t_-) \tag{7}$$

where e_{res} is the restitution coefficient and t_- and t_+ is the plate velocity immediately before and after impact respectively.

The spring actuating force, F_{act}, is determined by:

$$F_{act} = C_f A_p \Delta\mathrm{P} \tag{8}$$

where A_p is the area of the port, ΔP is the change in pressure, and C_f is a force coefficient which is determined empirically or by use of Böswirth's model [53], [63], [68], [69]. The force coefficient can be determined with Eq. (9) if the valve entrance friction is known:

$$C_f = \frac{1}{1 + \mathrm{B}} \tag{9}$$

where B is determined with:

$$\mathrm{B} = \xi\left(\frac{A_o\, C_d}{A_p}\right)^2 \tag{10}$$

and where ξ is the valve entrance friction coefficient and A_o is the valve opening area, otherwise $C_f \approx 1$ [69].

2.5 Compressor valve mass flow modelling

Researchers have modelled the mass flow of the working fluid through a valve for various reasons. One basis for study is the reduction of noise created by gas pulsations when the working fluid moves though the valve into the suction or discharge plenum [70], [71]. Another reason for modelling valves studies the effect of valve dynamics on compressor efficiency [67].

The calculation of the mass flow rate through a valve is dependent on the Mach number of the working fluid. A Mach number exceeding 0,3 influences the density of the fluid, which in turn influences the mass flow rate [68].

For steady, incompressible flow (Mach < 0,3), authors base their models on flow through an orifice of equivalent size to the valve opening [66], [67], [70], [72]. Srinivas et al. [70] accounted for the nonidealities of valve movement due to a change in pressure that results in gas leakage, where the valve does not exhibit instantaneous opening or closing but deceleration, stopping, and a change in direction. The mass flow through an orifice is modelled with:

$$\dot{m}_s = \begin{cases} C_{D_s}\rho_s A_{sv}\sqrt{\dfrac{2(P_s - P_i)}{\rho_s}}, for\ P_s > P_i\ and\ x_s > 0 \\ -C_{D_s}\rho_i A_{sv}\sqrt{\dfrac{2(P_i - P_s)}{\rho_i}}, for\ P_i > P_s\ and\ x_s > 0 \end{cases} \tag{11}$$

$$\dot{m}_d = \begin{cases} C_{D_d}\rho_i A_{dv}\sqrt{\dfrac{2(P_i - P_d)}{\rho_i}}, for\ P_i > P_d\ and\ x_d > 0 \\ -C_{D_d}\rho_d A_{dv}\sqrt{\dfrac{2(P_d - P_i)}{\rho_d}}, for\ P_d > P_i\ and\ x_d > 0 \end{cases} \tag{12}$$

where $C_{D_s}$and C_{D_d} are the discharge coefficients, ρ_i, ρ_s and ρ_d are instantaneous, suction, and discharge densities, A_{sv} and A_{dv} are the suction and discharge valve flow areas, and x_s and x_d are the instantaneous valve displacement heights for the suction and discharge valve plates respectively.

For steady, compressible flow (0,3 < Mach < 0,8), authors base their models on flow through a nozzle [63], [68]. The Saint-Venant equation is used to calculate flow through the nozzle [53], [67], [68], [72]:

$$\dot{m} = A_{eff}\, \rho_1 \left(\frac{P_2}{P_1}\right)^{\frac{1}{\gamma}} \sqrt{2\frac{\gamma - 1}{\gamma}\left(1 - \frac{P_2}{P_1}^{\frac{\gamma-1}{\gamma}}\right)} \tag{13}$$

where A_{eff} is the effective valve area, ρ_1 is the upstream working fluid density, P_2 and P_1 are the down- and upstream pressures respectively, and γ is the specific heat ratio.

At certain velocities, the working fluid is chocked (Mach > 1), which creates a critical pressure ratio that replaces P_2/P_1 [53], [68], [72]:

$$\frac{P_{critical}}{P_1} = \frac{2}{\gamma + 1}^{\frac{\gamma}{\gamma-1}} \tag{14}$$

2.6 Overview of the modelling process

Compressors and their components are modelled to identify areas of energy use, the influence of design changes, and compressor performance. Various methods of modelling are used to simulate reciprocating compressors with varied complexity.

Mathematical models are categorised in the literature based on various characteristics. Rasmussen and Jakobsen [73] categorise mathematical models according to the complexity of creating the model. The following six categories were created:

- Statistical correlations based on the system performance
- Statistical correlations based on the compressor performance variables
- Process-oriented models
- Phenomena-oriented models with one or more control volumes
- Construction-oriented models with many control volumes and dynamic models
- Distributed models which use partial differential equations

2.6.1 Empirical models

Empirical models, which encompass both statistical correlation model types, are basic mathematical models created from experimental datasets. This type of model requires a large quantity of input data, which is usually only available to the compressor manufacturer. The data is used to plot compressor performance, which enables the creation of polynomial curve equations to simulate the compressor system [70], [73], [74], [75].

Empirical models are primarily used for fault-finding or supplied by the compressor manufacturers to clients for product selection [73]. Empirical models are also used for testing conditions set by ISO, ASHRAE, AHRI, etc. [73].

Alternatively, basic thermodynamic correlations can also be used to calculate compressor output conditions. These semi-empirical models require less experimental input data as they are created with well-known thermodynamic properties [74], [76]. This enables researchers to simulate compressors without extensive experimental data known only to the manufacturers.

2.6.2 Process-oriented models (zero-dimensional models)

Process-oriented models are of increased complexity when compared to empirical and semi-empirical models, as the compressor system is divided into different subprocesses, each modelled separately [73].

Bradshaw et al. [77] described a comprehensive compressor model which required inputs from five submodels of various compressor components and parameters. Similarly, Yang et al. [78] simulated compressor valve springs, while Boswirth et al. [79] modelled compressor valves to enable the designer to predict valve flutter.

The process of compression, occurring inside the compressor cylinder, is also simulated separately [52], [70], [80], [81]. The modelling of the compression process can be divided into two groups, a polytropic compression process and an energy process, where the first law of thermodynamics is used [82].

Various researchers have successfully modelled and validated the compression process as a polytropic process [52], [70], [80]. Lee et al. [83] compared a polytropic model, with different polytropic indexes, to a model where the first law is used. This comparison showed that the polytropic process model is a suitable substitute for the more complex first law process model, with the only shortcoming being the modelling of instantaneous temperature [83].

2.6.3 One-dimensional (1D) and two-dimensional (2D) models

1D or phenomena-oriented models of reciprocating compressors include the modelling of one or multiple control volumes. 1D models focus on simulating phenomena inside the compressor instead of focusing on individual components [73].

Winandy et al. [75] successfully created a simplified 1D model following detailed experimental analysis of a reciprocating compressor. The author was able to accurately calculate the mass flow rate, mechanical power, and discharge temperature from the 1D model [75].

Rasmussen and Jakobsen [73] further explain that, as the number of individual control volumes in the model increase, the control volumes tend to represent individual components.

Mohammadi-Amin et al. [84] compared a process-oriented model with a 2D model and found good agreement between the resulting data. They conducted a parametric study of the compressor with the 0D model results as input for the more sophisticated 2D model.

Aigner et al. created both a 1D and 2D model to calculate the effect of pressure waves on valve dynamics [85]. The models showed good agreement with experimental data and were thus deemed sufficient to capture main compressor characteristics.

Balduzzi et al. [86] described a simplified 2D modelling strategy to accurately simulate a reciprocating compressor. The use of this strategy eliminated the need for a 3D model, resulting in reduced simulation costs.

The literature has shown that researchers have opted for less complex 0D, 1D, and 2D models compared to complex and costly 3D models [67], [82], [84], [85], [86], [87].

2.6.4 Three-dimensional (3D) models

With advancement in the computational power of computers, researchers have been able to simulate compressors in three dimensions [25]. These 3D models make use of partial differential equations to accurately simulate multiple processes in multiple volumes. The interaction between fluids and devices can also be simulated using Computational Fluid Dynamics (CFD). CFD modelling is the most detailed modelling method available but requires substantial modelling and computational effort [87].

Suh et al. [88] and Pereira et al. [89] have successfully created simplified 3D models of individual compressor components as an alternative to full 3D compressor simulation. Ferreira et al. [90] created a full CFD model of a reciprocating compressor to simulate heat transfer but noted that the simulation was computationally expensive. Various authors have developed hybrid models, where complex processes are modelled with CFD and less complex processes with process models to save computational cost [91].

Process-oriented models have been used to adequately simulate various phenomena of a reciprocating compressor when compared to equivalent 1D, 2D, and 3D models [87], [92]. The process-oriented models have shown good agreement with experimental results with the benefit of requiring less computational power and effort.

2.7 Summary

In this chapter, the different compression processes were discussed, and various methods of achieving quasi-isothermal compression were investigated. The improvement of compressor efficiency through various cooling methods was discussed. External and internal cooling methods were described, while emphasis was placed on in-cylinder coolant injection.

Different cylinder wall heat transfer correlations were investigated and summarised in Table 1. Work by various authors was studied, and it was found that Adair et al.'s correlation is widely used (see Table 2).

The different types of valves utilised in compressors were discussed with accompanying equations for modelling the valve dynamics. The effect of the Mach number on valve mass flow was investigated, and three equations were listed for incompressible, compressible, and chocked flow.

The different modelling processes, from empirical to 3D models, were discussed, and a first law model for simulating a reciprocating compressor with coolant injection and suction valve control was deemed suitable for implementation in this study.

2.8 Conclusion

In-cylinder coolant injection process-oriented models have shown good agreement with experimental results [52], [93]. The use of a polytropic index for modelling the compression process is widely used in literature [52], [70], [80]. The first law of thermodynamics can also be used to model the compression process. It is relatively simple to implement and enables instantaneous temperature modelling of the compression process, which is desirable when modelling the effect of in-cylinder cooling [83].

The increased accuracy pertaining to the modelling of instantaneous temperature with a first law model has made it a good candidate for simulating in-cylinder coolant injection with suction valve control.

Chapter 3: Modelling and simulation of reciprocating compressor with coolant injection and valve control

3.1 Introduction

This section describes a first law of thermodynamics mathematical model of a reciprocating compressor. A single-cylinder, single-acting compressor is considered with the assumption that the model employed will be applicable to multicylinder compressors as well.

A basic schematic of the compressor model is shown in Figure 9. The working fluid enters the cylinder through the suction valve at a mass flow rate of $\dot{m}_s$, temperature T_s, and pressure P_s, while leaving through the discharge valve at a mass flow rate of $\dot{m}_d$, temperature T_d, and pressure P_d. It is assumed that no spatial variation in pressure or temperature is present inside the cylinder and piston ring leakage, and other nonidealities are ignored.

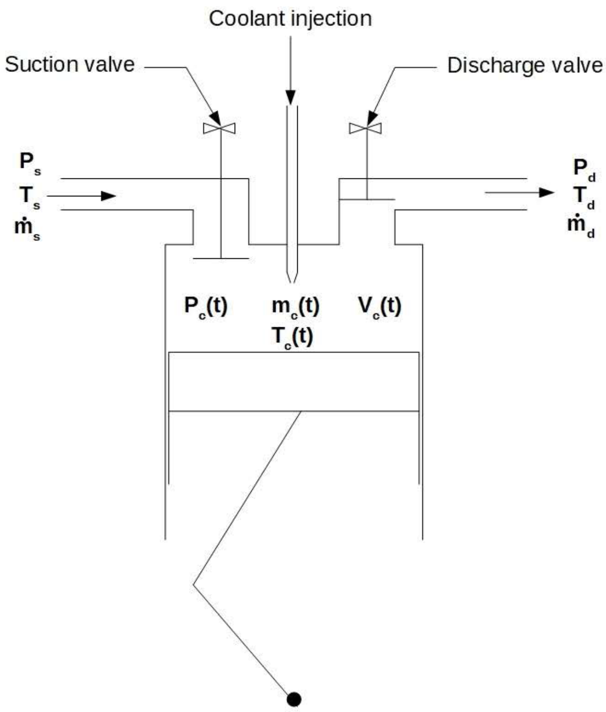

Figure 9: Schematic of compressor model

3.2 First law modelling of a reciprocating compressor

The compression and expansion processes are modelled using the first law of thermodynamics (*cf.* Eq. (1)). The model created for this study is based on the thermodynamic model used by Singh et al. [94] which was used to simulate an oil-flooded twin-screw compressor.

Repeated here from Chapter 2 for convenience is equation (1), the first law of thermodynamics, which states that the change in internal energy (ΔU) is equal to the change in the work done (W) on the system and the heat energy (Q) which is either generated or rejected.

$$\Delta U = W - Q \tag{1}$$

The internal energy term can be written in the time interval Δt as:

$$\frac{dU}{dt} = C_v \left[\frac{dm}{dt}T + (T - T_s)\dot{m}_s\right] \tag{15}$$

where C_v is the specific heat capacity at constant volume of the working fluid, dm/dt the mass rate of change of the working fluid inside the cylinder, T the temperature of the working fluid, T_s the temperature of the working fluid through the suction valve, and $\dot{m}_s$ the mass flow rate through the suction valve.

The work term can be written as:

$$\frac{dW}{dt} = P\frac{dV}{dt} - \frac{P_s}{\rho_s}\dot{m}_s + \frac{P}{\rho}\dot{m}_d \tag{16}$$

where P is the instantaneous pressure inside the cylinder, dV/dt the rate of change of volume, ρ the working fluid density, and $\dot{m}_d$ the mass flow rate through the discharge valve.

The assumption is made that the working fluid is a perfect gas, thus, eq. (1) can be rewritten when combining (1), (15), and (16) as:

$$\dot{Q} = C_v \left[\frac{dm}{dt}T + (T - T_s)\dot{m}_s\right] + P\frac{dV}{dt} - \frac{P_s}{\rho_s}\dot{m}_s + \frac{P}{\rho}\dot{m}_d \tag{17}$$

The mass relationship can be expressed as:

$$\frac{dm}{dt} = \dot{m}_s - \dot{m}_d \tag{18}$$

And the ideal gas law as:

$$PV = mRT \tag{19}$$

where R is the gas constant.

Thus, using equations (18) and (19), equation (17) can be reduced to:

$$\frac{dP}{dt} = \frac{\gamma - 1}{V}\dot{Q} - \frac{\gamma P}{V}\frac{dV}{dt} - \frac{\gamma P}{\rho V}\dot{m}_d + \frac{\gamma}{V}\frac{P_s}{\rho_s}\dot{m}_s \tag{20}$$

The specific heat ratio γ can be expressed as:

Error! Bookmark not defined.

$$\gamma = \frac{C_p}{C_v} \tag{21}$$

where C_p is the specific heat capacity of the working fluid at constant pressure.

The gas constant can be expressed as:

$$R = C_p - C_v \tag{22}$$

Combining equations (21) and (22),

$$\frac{R}{C_v} + 1 = \gamma \tag{23}$$

Heat transfer through the cylinder wall can be expressed as [1]:

$$\dot{Q} = h_w A(T_w - T) \tag{24}$$

where h_w is the coefficient of heat transfer of the cylinder wall, A the total area of the cylinder wall in contact with the working fluid, T_w the instantaneous cylinder wall temperature, and T the cylinder gas temperature.

The coefficient of heat transfer for this simulation was calculated by solving Woschni et al.'s [55] equation. Woschni's correlation was selected, as it was found to be the median of the compared correlations, as can be seen from the graphs of Tuhovcák et al. [60], and for its low computational cost. Woschni et al.'s correlation is determined with:

$$h_w = 0.035(R_e)^{0.8} \tag{25}$$

where the Reynolds number is calculated with:

$$R_e = \frac{vD_{cyl}}{\mu} \tag{26}$$

where D_{cyl} is cylinder diameter, μ the working fluid kinematic viscosity, and v the characteristic velocity in m/s. For open valves, $v = 6.618 \times v_{piston}$ and for closed valves, $v = 2.28 \times v_{piston}$.

Combining equations (19), (20), (23), and (24), the instantaneous cylinder pressure can be calculated with:

$$\frac{dP}{dt}=\frac{R\gamma}{V}(\dot{m}_sT_s-\dot{m}_dT)+\frac{Rh_wA_w}{C_vV}(T_w-T)-\frac{dV}{dt}\frac{P}{V}\left(\frac{R}{C_v}+1\right) \tag{27}$$

3.2.1 Modelling of cylinder volume rate of change

The compressor to be modelled is assumed to be crank driven. Srinivas et al. [70] expressed an equation to describe a crank-driven compressor's cylinder volume at any moment as:

$$V=V_{cle}+\frac{V_{str}}{2}[1-\cos(\omega t)] \tag{28}$$

where V is cylinder volume, V_{cle} cylinder clearance volume, V_{str} stroke volume, ω crank angular velocity, and t time. Solving equation (27) requires the rate of change in compressor volume, dV/dt, which can be found by differentiating equation (28):

$$\frac{dV}{dt}=\frac{V_{str}}{2}\omega\sin(\omega t) \tag{29}$$

3.2.2 Modelling mass flow through valves

To determine the mass flow rate through the valves in this simulation, the approach set forth by Srinivas et al. [70] will be used (*cf.* Eq. (11) and (12)). This approach was chosen to minimise the computational cost and account for both valve nonidealities and back flow.

$$\dot{m}_s=\begin{cases}C_{D_s}\rho_sA_{sv}\sqrt{\dfrac{2(P_s-P_i)}{\rho_s}}, for\ P_s>P_i\ and\ x_s>0\\ -C_{D_s}\rho_iA_{sv}\sqrt{\dfrac{2(P_i-P_s)}{\rho_i}}, for\ P_i>P_s\ and\ x_s>0\end{cases} \tag{11}$$

$$\dot{m}_d=\begin{cases}C_{D_d}\rho_iA_{dv}\sqrt{\dfrac{2(P_i-P_d)}{\rho_i}}, for\ P_i>P_d\ and\ x_d>0\\ -C_{D_d}\rho_dA_{dv}\sqrt{\dfrac{2(P_d-P_i)}{\rho_d}}, for\ P_d>P_i\ and\ x_d>0\end{cases} \tag{12}$$

3.2.3 Modelling valve dynamics and suction valve control

The desired compression process for the model, developed in this study, includes a novel approach where quasi-isobaric compression is achieved at the commencement of the compression stroke, as described by Jacobs [53]. This process is followed by quasi-isothermal compression (*viz.* process 1-4-5 in Figure 6).

The suction valve is modelled as a simple valve that is either fully open or fully closed. This modelling approach allows the valve to be simulated as closed during the quasi-isobaric process. The suction valve dynamics is based on the experimental setup implemented by Jacobs [53].

The discharge valve will be assumed to be a poppet valve, and it will be modelled as a simple spring-mass-damper system. The working fluid is assumed to be incompressible (Mach < 0,3), thus following the approach set forth by Srinivas et al. [70] (*cf.* Eq. (6) and (7)). The restitution effect will be neglected in this model.

3.2.4 Modelling coolant injection with adiabatic mixing

Heat transfer in the compressor subjected to coolant injection occurs between (a) the working fluid (gas that is being compressed) and the cylinder wall, and (b) between the working fluid and the coolant.

The heat transfer from the working fluid to the cylinder wall is calculated with equation (24). If an isothermal or quasi-isothermal compression process is considered, heat transfer to the cylinder wall will be negligible.

Mixing of the working fluid and coolant is assumed to be an adiabatic mixing process, which was selected because the heat transfer from the cylinder to its surroundings is negligible, and the in-cylinder mixing process involves no work [24].

The change in energy for an ideal adiabatic mixing process can be expressed as:

$$\frac{dE_{cyl}}{dt} = \dot{E}_s + \dot{E}_c - \dot{E}_d \tag{30}$$

where $\dot{E}_s$ is the change in energy when the suction valve is open, $\dot{E}_c$ is the change in energy during coolant injection, and $\dot{E}_d$ is the change in energy when the discharge valve is open.

The change in energy can be expressed in terms of mass flow rate and specific enthalpy, $\dot{E} = \dot{m}h$, where specific enthalpy can also be written as $h = c_p T$. Thus, equation (30) can be expressed as:

$$\frac{\Delta m_{cyl} c_{p_{cyl}} T_{cyl}}{\Delta t} = \left(\dot{m}_s c_{p_s} T_s\right) + \left(\dot{m}_c c_{p_c} T_c\right) - \left(\dot{m}_d c_{p_d} T_d\right) \tag{31}$$

For a nonideal adiabatic mixing process, which better describes mixing in a compressor with coolant injection, an adiabatic mixing effectiveness factor can be defined. Similar to Khan et al. [95], who introduced the concept of quantifying the mixing effectiveness of flooded compressors, an adiabatic mixing effectiveness factor ranging from 0 (no mixing) to 1 (perfect mixing) can be used to account for nonideal adiabatic mixing compressors with coolant injection.

Equation (31) can be rewritten as:

$$\frac{\Delta m_{cyl} c_{p_{cyl}} T_{cyl}}{\Delta t} = \left(\dot{m}_s c_{p_s} T_s\right) + \left(\Phi \dot{m}_c c_{p_c} T_c\right) - \left(\dot{m}_d c_{p_d} T_d\right) \tag{32}$$

where Φ is the adiabatic mixing effectiveness factor.

To account for the adiabatic mixing effectiveness on in-cylinder temperature, and to ensure that the conservation of mass is upheld, the coolant mass flow in equation (18) is also multiplied with the effectiveness factor (Φ). Equation (18) can be rewritten as:

$$\frac{dm}{dt} = \dot{m}_s + \Phi\dot{m}_c - \dot{m}_d \tag{33}$$

To quantify the adiabatic effectiveness factor, a sensitivity analysis comparing simulated and experimental data will be conducted to determine its approximate value.

3.2.5 Modelling coolant mass

The coolant injected into the compressor cylinder influences not only the in-cylinder temperature but also the cylinder volume. A gaseous coolant will have a negligible effect on the cylinder volume, while a liquid, which is considered incompressible throughout this study, will decrease the cylinder volume when injected.

When a small amount of liquid coolant is injected into the cylinder, the liquid coolant will evaporate and create a vapour mixture. As more liquid coolant is injected, the mixture will become increasingly saturated with liquid until fully saturated, at which point the liquid coolant will not evaporate but exist as a liquid.

Although the vapour mixture will be discharged at the end of the cycle, the liquid will build up inside the compressor cylinder, as the clearance volume ensures that a certain amount of the vapour remains in the cylinder after each cycle. This liquid coolant build-up will decrease the cylinder volume and is accounted for with an empirically determined fraction.

Figure 10 illustrates how the clearance volume is affected by the build-up of the injected coolant. Line a-a depicts a dry expansion process, while line b-b depicts the expansion where the clearance volume is decreased due to the injected coolant not evacuating the clearance volume after each cycle.

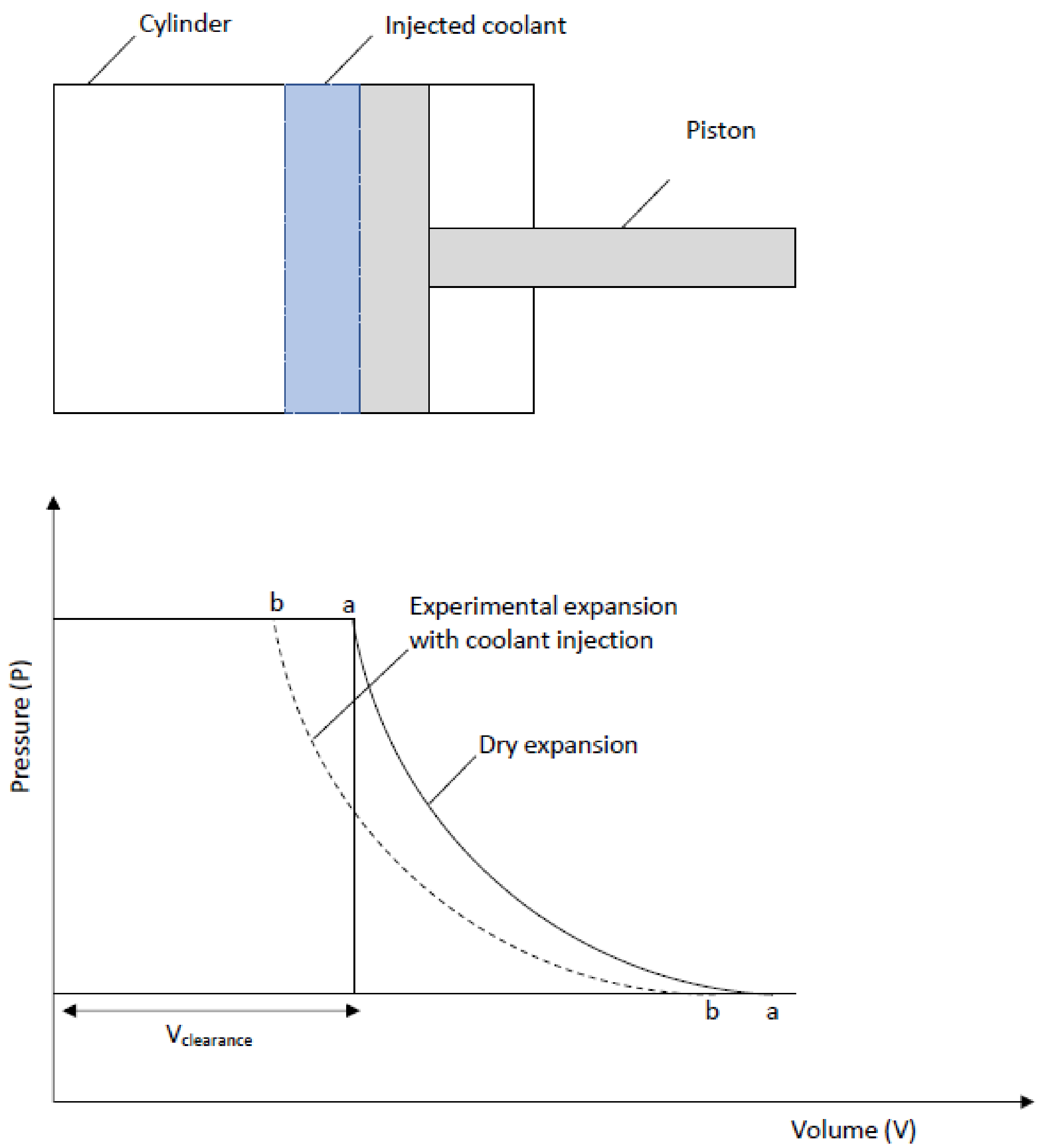

Figure 10: Clearance volume variance due to coolant injection

3.2.6 Modelling coolant mass flow rate

To simulate the mass flow rate of coolant injected during timed cooling cases, the mass flow rate was calculated using the measured coolant injection pressure. The coolant mass flow rate can be expressed as [citation?]:

$$\dot{m}_{coolant} = \rho_{water} \times C_d \times \left(\frac{\pi}{4} \times d_{nozzle}{}^2\right) \times \sqrt{\frac{(2 \times P_{inj})}{\rho_{water}}} \tag{34}$$

where ρ_{water} is the density of water at 15°C, C_d the coefficient of discharge of the nozzle, d_{nozzle} the diameter of the nozzle, and P_{inj} the injection pressure of the coolant. The diameter of the nozzle was 0.3 mm, and the average injection pressure 5 MPa, obtained from Jacobs [53].

The nozzle coefficient of discharge C_d is unknown; therefore, a sensitivity analysis comparing the simulated and experimental data will be conducted to determine the influence of C_d on compressor performance. The C_d will be calibrated against the experimental results to obtain an approximate coefficient of discharge C_d.

3.3 First law model and simulation initial inputs and outputs

The initial input values of certain model parameters necessary to numerically simulate the compressor was selected and based on the input values used by Jacobs [53]. The initial input parameters can be changed within the model to simulate different compressor setups and scenarios. These parameters were used to investigate the effect of in-cylinder coolant injection with suction valve control on a reciprocating compressor.

General initial inputs

- Compressor rotational speed (N)
- Stroke length (L_{str})
- Cylinder internal diameter (D_{cyl})
- Percentage clearance volume ($V_{cle\%}$)
- Discharge pressure (P_d)
- Suction pressure (P_s)
- Suction temperature (T_s)
- Cylinder wall temperature (T_w)
- Discharge temperature (T_d)
- Compressor mass flow without coolant injection ($\dot{m}_{DRYRUN}$)
- Coolant mass flow as a fraction of compressor mass flow ($\dot{m}_{coolant}$)

Model options

1. Valve options
   a. Automatic plate valves
   b. Simple check valves
   c. Timed valves
   d. Timed valves with cooling
   e. Timed suction valve with cooling and automatic discharge poppet valve
2. Cooling options
   a. Continuous cooling
   b. Timed cooling

3.4 Solution algorithm

The equations given above are classified as first- and second-order nonlinear ordinary differential equations (ODEs). This system of differential equations must be solved simultaneously to simulate the workings of the compressor.

The fourth-order Runge-Kutta method was chosen to solve these equations for its ease of implementation. The formula to solve ODEs with the Runge-Kutta method is:

$$\begin{aligned} K_1 &= f(t_i,\, y_i) \\ K_2 &= f\left(t_i + \frac{\Delta t}{2},\, y_i + \frac{\Delta t}{2} K_1\right) \\ K_3 &= f\left(t_i + \frac{\Delta t}{2},\, y_i + \frac{\Delta t}{2} K_2\right) \\ K_4 &= f(t_i + \Delta t,\, y_i + \Delta t K_3) \\ Y_{i+1} &= y_i + \frac{\Delta t}{6}(K_1 + 2K_2 + 2K_3 + K_4) \end{aligned} \tag{35}$$

3.5 where t is the time, subscript i the step, Δt the time-step size, and y the variable to be solved. The Runge-Kutta method can be used to solve multiple ODEs simultaneously by simply adding the applicable variables to the function.Summary

This section described the first law of thermodynamics mathematical model of a reciprocating compressor. This model can be used to simulate a reciprocating compressor either with or without coolant injection to achieve quasi-isothermal compression. This model can also simulate a quasi-isobaric process at the commencement of the compression stroke followed by quasi-isothermal compression.

The following chapter will present and discuss the results obtained from the numerical simulation. The results will be compared with the experimental results obtained by Jacobs [53] which will serve as validation of the first law of thermodynamics mathematical model developed in this study.

Chapter 4: Numerical simulation and validation

4.1 Introduction

In this chapter, the results from the numerical simulation developed in Chapter 3: will be presented and discussed. The results from the numerical simulation are compared with the experimental results obtained by Jacobs [53]. This comparison will serve as the validation of the first law of thermodynamics mathematical model presented in Chapter 3:.

4.2 Simulation methodology

This simulation is implemented in Mathcad Prime 8.0.0.0. software. The fluid properties used were ascertained by means of Engineering Equation Solver (EES) software. Multiple data points were exported to a Mathcad worksheet, and a curve fit was generated. The resulting equation was referenced in the mathematical model.

4.3 Description of validation cases

Jacobs [53] experimentally measured six criteria during eight test cases. The test groups consisted of a test case without cooling and one with timed cooling at a target pressure ratio of 4, a test case without cooling, one with timed cooling, two with continuous cooling at a target pressure ratio of 5.5, a test case without cooling, and one with timed cooling at a target pressure ratio of 7. The parameters measured were suction pressure, discharge pressure, suction temperature, discharge temperature, coolant temperature, and compressor speed (*cf.* Table 3). The experimental values of the parameters from Jacobs [53] were used as the input values for the numerical simulation presented here. The experimental data and simulated results were quantifiably compared (*cf.* Figure 11 and Figure 14) with tolerance limits similar to those used by Jacobs [53].

Jacobs [53] utilised functional analysis to quantify the difference between experimental and modelled data. The Euclidean Relative Difference (ERD), Euclidean Projection Coefficient (EPC), and Secant Cosine (SC) were used. The ERD evaluates the average difference between the experimental and model data; thus, an ERD value of zero would suggest a perfect curve fit. The EPC is a factor which would provide a perfect curve fit between the modelled and experimental data when multiplied by the experimental data. An EPC of 1 would result in a perfect curve fit. SC evaluates the fit of the modelled data curve according to its shape relative to the shape of the experimental data curve. A perfect shape fit would render an SC of 1.

The tolerance limit used during validation is 20%, suggesting that the modelled data does not deviate further than $ERD \leq 0.2, 0.8 \leq EPC \leq 1.2,$ and $SC \geq 0.8.$

Table 3: Summary of experimental data obtained by Jacobs [53]. Used as input data for the numerical simulation.

Test group	Suction pressure (kPa)	Discharge pressure (kPa)	Suction temperature (˚C)	Discharge temperature (˚C)	Coolant temperature (˚C)	Pressure ratio	Speed (r/min)
4 Dry	86.4	349.5	45.2	96.7	-	4.1	475.2
4 Timed	87.0	364.6	44.8	60.7	15.3	4.2	489.1
5.5 Dry	86.4	493.2	45.0	99.9	-	5.7	465.1
5.5 Timed	84.2	489.0	44.7	59.0	14.3	5.7	484.1
7 Dry	86.9	602.2	44.8	103.2	-	6.9	460.2
7 Timed	87.2	593.0	44.8	60.5	12.3	6.8	483.1

Table 4: Experimental data measurement uncertainty from [53]

Measurement	Range	Uncertainty (95% confidence)(1)
Suction pressure	0 – 100 kPa a	± 1.03 kPa (± 1.03% of FS)
Discharge pressure	0 – 1 600 kPa a	± 16.34 kPa (± 1.02% of FS)
Cylinder pressure	0 – 1 600 kPa a	± 8.66 kPa (± 0.54% of FS)
Coolant injection pressure	0 – 10 000 kPa a	± 54.15 kPa (± 0.54% of FS)
Suction temperature	-10 - 50°C	± 0.51 °C (± 1.02% of FS)
Discharge temperature	0 - 360°C	± 3.61 °C (± 1.00% of FS)
Coolant injection temperature	-10 - 50°C	± 0.51 °C (± 1.02% of FS)
Shaft position	0 - 360°C	± 0.51 °C (± 0.51% of FS)

(1) Expanded uncertainty with coverage factor of 2 gives 95% confidence level. Measurement uncertainty includes influence of instrument and data acquisition system (kPa a, absolute pressure in kPa; FS, full-scale).

A Type B uncertainty analysis as defined by NIST and ISO was used by Jacobs [53] to determine uncertainties of measurement.

4.4 Coolant injection nozzle coefficient of discharge sensitivity analysis

As discussed in 3.2.6, a sensitivity analysis was conducted where the coefficient of discharge C_d varied between 0.3 and 0.6 for all timed coolant injection cases. The C_d limit range was based on the findings of [96], who found that the C_d varies between 0.3 and 0.6 for hydraulic swirl nozzles. It is evident in Table 4 that $C_d = 0.3$ shows the best comparison with experimental data for all timed coolant injection cases. Therefore, a coefficient of discharge of 0.3 will be used during all validation cases.

Table 5: Coefficient of discharge sensitivity analysis results

Test group	Cd	ERD[(a)]	EPC[(b)]	SC[(c)]
4 Timed coolant injection	0.3	0.134	1.024	0.973
	0.4	0.135	1.027	0.973
	0.5	0.136	1.030	0.972
	0.6	0.138	1.033	0.972
5.5 Timed coolant injection	0.3	0.136	1.064	0.982
	0.4	0.137	1.066	0.982
	0.5	0.138	1.067	0.982
	0.6	0.139	1.069	0.982
7 Timed coolant injection	0.3	0.133	1.091	0.986
	0.4	0.134	1.092	0.986
	0.5	0.135	1.093	0.986
	0.6	0.135	1.094	0.986

[(a)] ERD: Average difference between experimental and model data. Perfect fit: ERD = 0
[(b)] EPC: Quality of curve fit of model data compared to experimental data: Perfect fit: EPC = 1
[(c)] SC: Quality of modelled data shape compared to experimental data. Perfect fit: SC = 1

Figure 11 and Figure 12 shows the temperature curve for each coefficient of discharge for the 4 timed case. A reference case, where $C_d = 1$, was also included for illustration purposes. These curves confirm that the model is sensitive to a change in coefficient of discharge, and that the coefficient of discharge influences the discharge temperature.

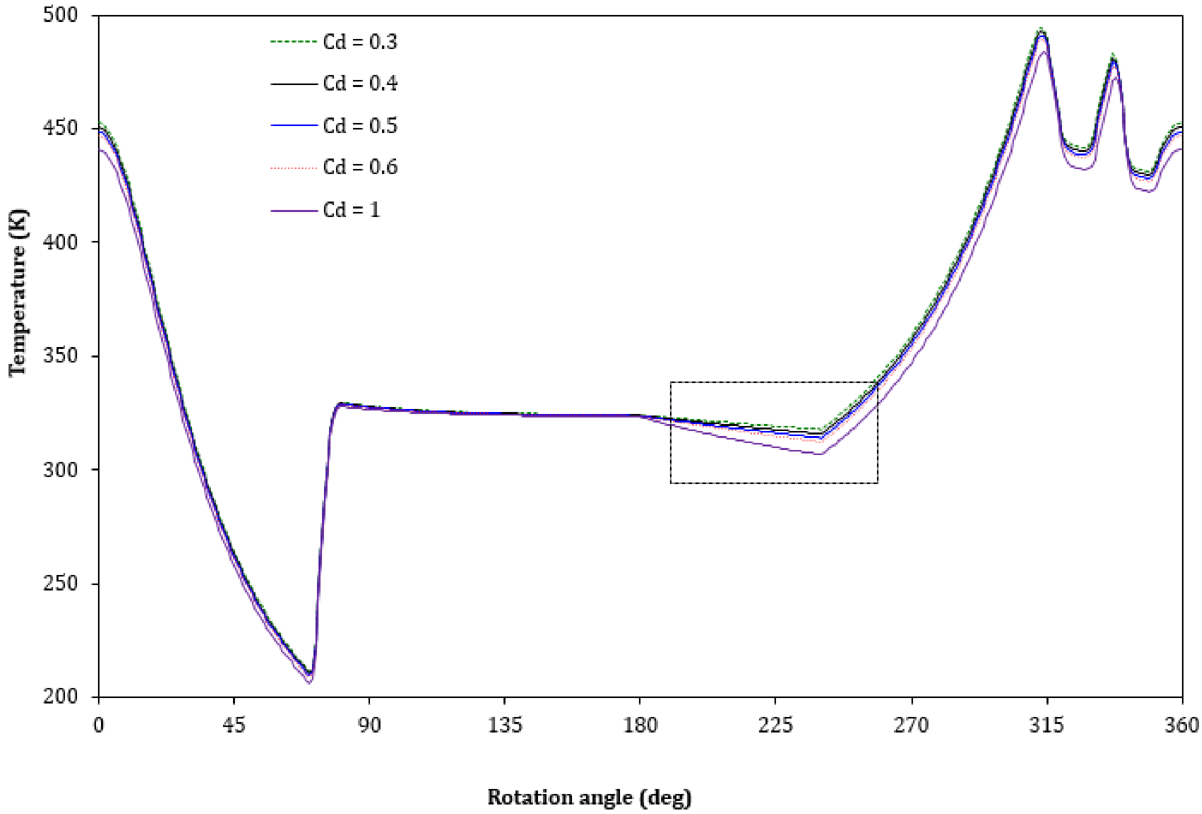

Figure 11: Temperature comparison between different coefficients of discharge cases

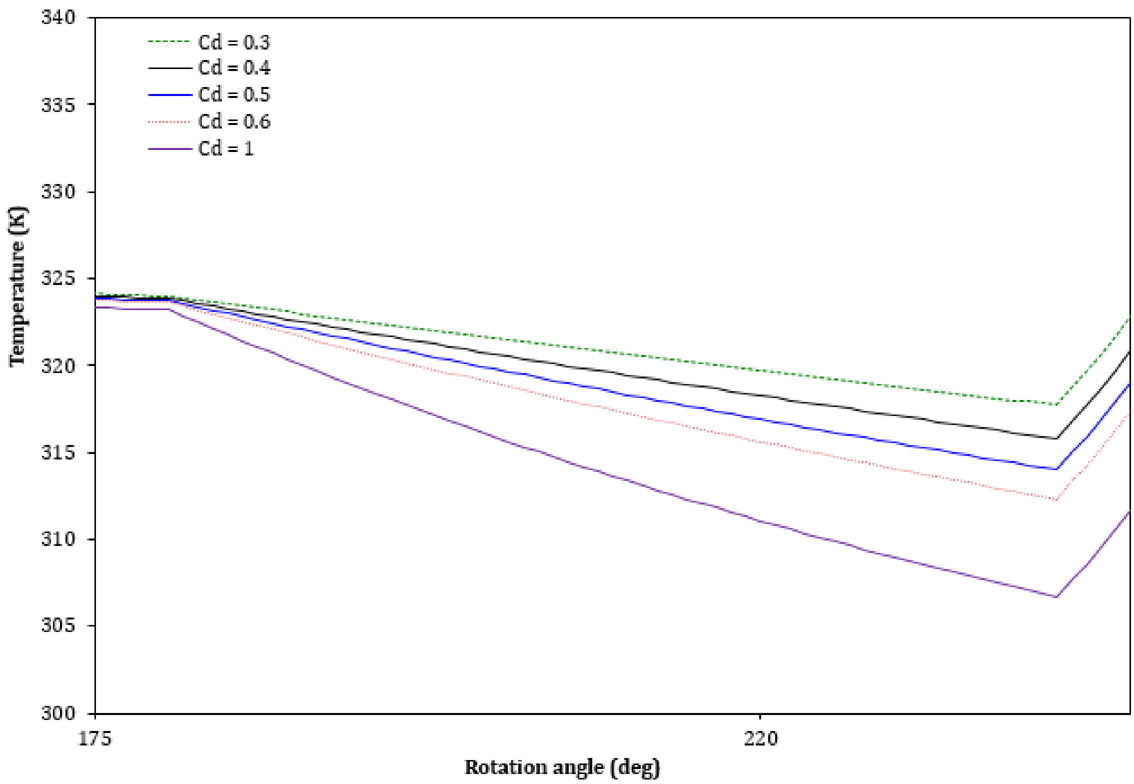

Figure 12: Enlarged area as shown in Figure 11

4.5 Effect of cylinder wall temperature

The cylinder wall temperature (T_{wall}) was varied to determine its effect on cylinder pressure. The 4 dry simulated case was used where the cylinder wall temperature was simulated as being equal to the suction, discharge, and mean air temperatures. Table 5 shows the effect of the cylinder wall temperature on the validation results. It can be seen that the cylinder wall temperature has little to no effect on the simulated data when compared with the experimental results.

Table 6: Effect of cylinder wall temperature on validation results

Test case	T_{wall}	ERD[(a)]	EPC[(b)]	SC[(c)]
4 Dry	$T_{wall} = T_s$	0.227	1.132	0.910
	$T_{wall} = \frac{(T_s + T_d)}{2}$	0.227	1.133	0.910
	$T_{wall} = T_d$	0.228	1.134	0.910

[(a)] ERD: Average difference between experimental and model data. Perfect fit: ERD = 0
[(b)] EPC: Quality of curve fit of model data compared to experimental data: Perfect fit: EPC = 1
[(c)] SC: Quality of modelled data shape compared to experimental data. Perfect fit: SC = 1

4.6 Coefficient of heat transfer sensitivity analysis

The coefficient of heat transfer (h_w) determined with equation (25) was used to simulate the heat loss through the cylinder wall. This heat transfer coefficient is not representative of the experimental setup used by Jacobs [53]. Therefore, a calibration factor (CF_w) was introduced to correct the simulated results.

The dry simulated cases were used where the calibration factor was increased until the simulated and experimental discharge temperatures were within acceptable error limits. It was found that a calibration factor of 10.5 for the pressure ratio of 4, 21.5 for the pressure ratio of 5.5, and 25.5 for the pressure ratio of 7 should be used (*cf.* Table 6).

Table 7: Effect of coefficient of heat transfer calibration factor on discharge temperature

Test case	Experimental discharge temperature (K) [°C]	CF_w	Simulated discharge temperature (K) [°C]	Error percentage (%)
4 Dry	369.9 [96.7]	1	453.5 [180.4]	23
		18	370.1 [97]	0.1
5.5 Dry	373.1 [99.9]	1	510.3 [238.4]	37
		21.5	373.8 [100.7]	0.2
7 Dry	376.4 [103.2]	1	529.6 [256.5]	41
		25.5	377.5 [104.4]	0.3

4.7 Adiabatic mixing factor sensitivity analysis

As discussed in 3.2.4, an adiabatic mixing effectiveness factor (Φ) sensitivity analysis was conducted, as the effect of this factor is unknown. Table 7 shows the effect of the adiabatic mixing effectiveness factor when varied from 20% to 100% effectiveness. A $C_d = 0.3$ and mean cylinder wall temperature was used.

It can be seen from Table 7 that a lower adiabatic mixing effectiveness factor of 0.2 compares best with the experimental results for all test groups.

Table 8: Effect of adiabatic effectiveness factor on validation results

Test groups	Adiabatic mixing effectiveness Φ	ERD[a]	EPC[b]	SC[c]
4 Timed coolant injection	0.2	0.131	1.014	0.973
	0.4	0.132	1.017	0.973
	0.6	0.133	1.019	0.973
	0.8	0.133	1.021	0.973
	1	0.134	1.024	0.973
5.5 Timed coolant injection	0.2	0.134	1.058	0.982
	0.4	0.134	1.059	0.982
	0.6	0.135	1.061	0.982
	0.8	0.136	1.062	0.982
	1	0.136	1.064	0.982
7 Timed coolant injection	0.2	0.131	1.087	0.986
	0.4	0.131	1.088	0.986
	0.6	0.132	1.089	0.986
	0.8	0.132	1.090	0.986
	1	0.133	1.091	0.986

[a] ERD: Average difference between experimental and model data. Perfect fit: ERD = 0
[b] EPC: Quality of curve fit of model data compared to experimental data: Perfect fit: EPC = 1
[c] SC: Quality of modelled data shape compared to experimental data. Perfect fit: SC = 1

The low adiabatic mixing effectiveness factor can be attributed to two factors: insufficient penetration of the coolant into the cylinder during injection, or insufficient heat transfer between the coolant droplets and working fluid due to large average droplet sizes.

4.8 Validation results

The validation of the simulation was carried out with input parameters as per Table 3. A coefficient of discharge for the coolant injection nozzle of 0.3 for timed cases, a mean cylinder wall temperature calculated with the suction and discharge temperatures, and an adiabatic mixing factor of 0.2 was used for all simulated cases.

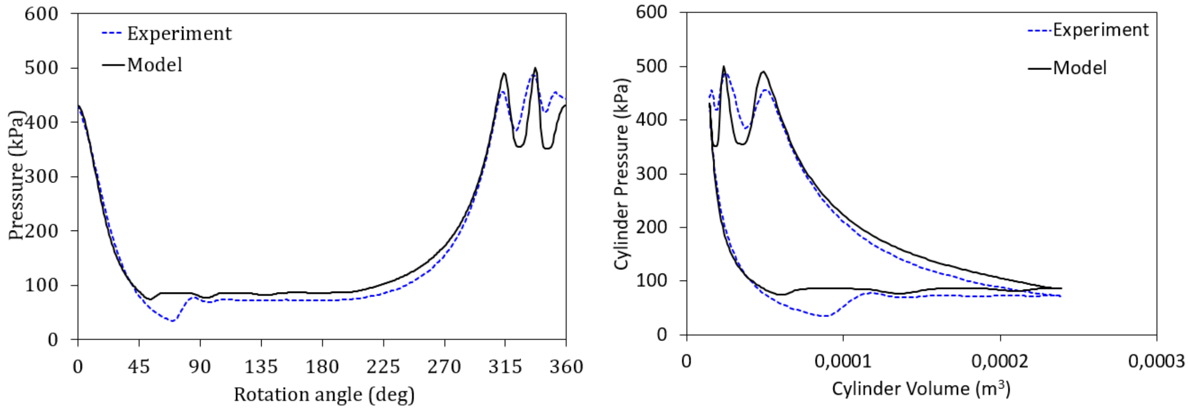

(a) Test case: 4 Dry

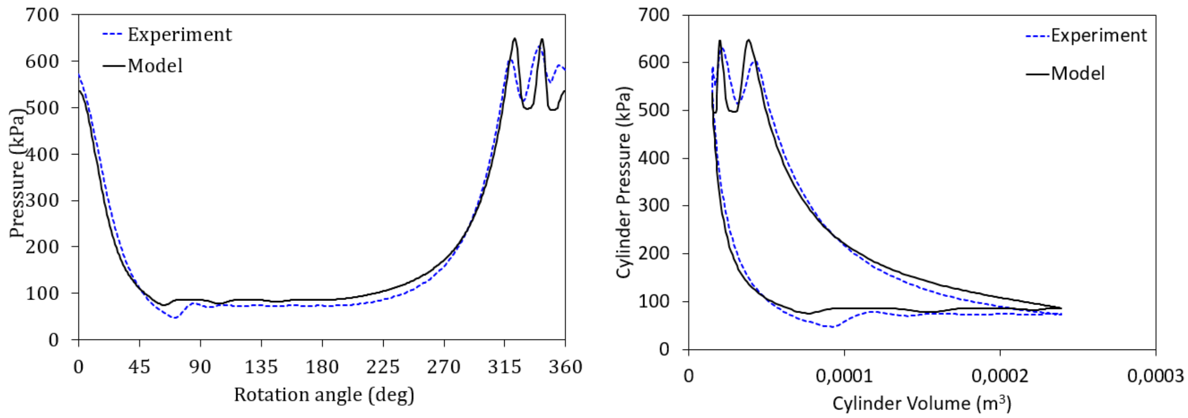

(b) Test case: 5.5 Dry

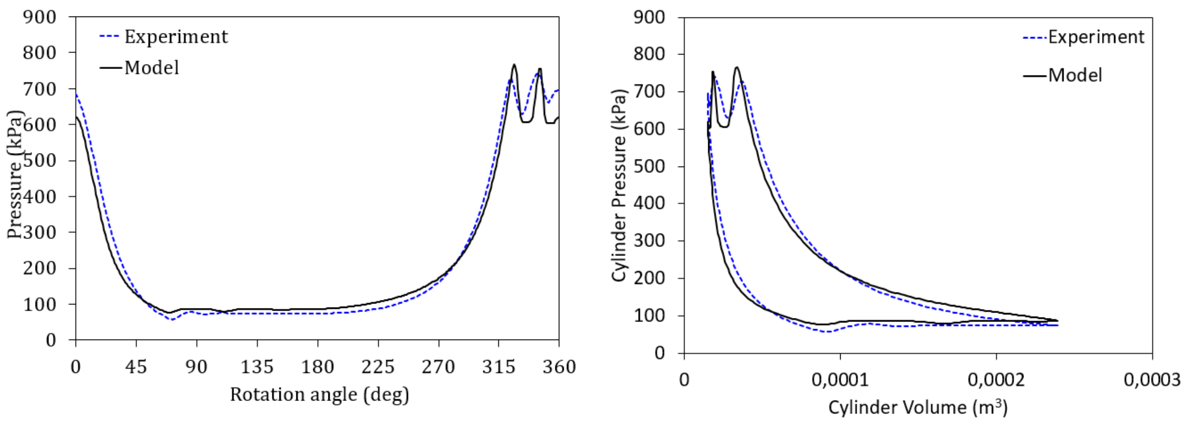

(c) Test case: 7 Dry

Figure 13: Dry validation cases data comparison

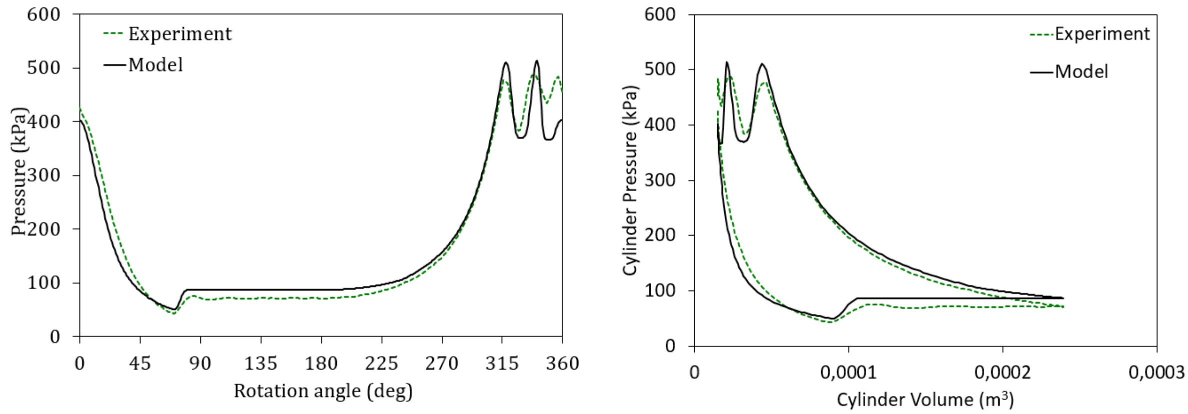

(a) Test case: 4 Timed

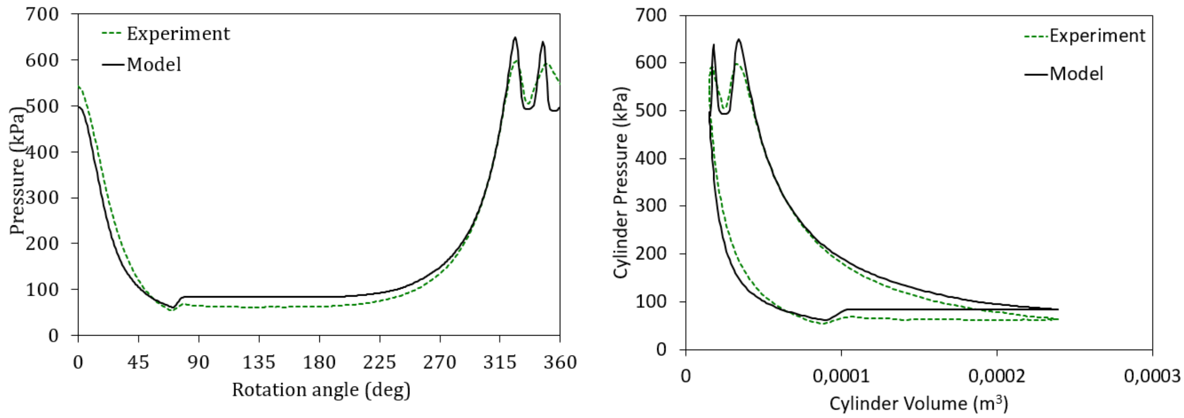

(b) Test case: 5.5 Timed

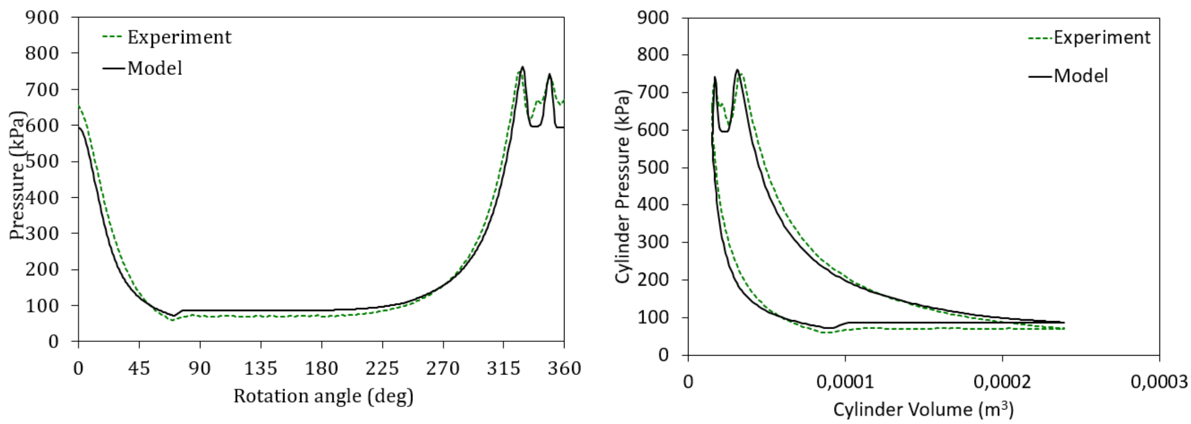

(c) Test case: 7 Timed

Figure 14: Timed P1 validation cases data comparison

Table 9: Validation results

Test group	ERD[(a)]	EPC[(b)]	SC[(c)]
4 Dry	0.124	0.974	0.952
4 Timed coolant injection	0.139	1.080	0.969
5.5 Dry	0.101	1.054	0.976
5.5 Timed coolant injection	0.141	1.102	0.985
7 Dry	0.133	1.118	0.984
7 Timed coolant injection	0.131	1.107	0.989
Maximum deviation	0.141	1.118	0.952
Average deviation	0.128	1.073	0.976
Minimum deviation	0.086	0.993	0.989

[(a)] ERD: Average difference between experimental and model data. Perfect fit: ERD = 0
[(b)] EPC: Quality of curve fit of model data compared to experimental data: Perfect fit: EPC = 1
[(c)] SC: Quality of modelled data shape compared to experimental data. Perfect fit: SC = 1

The results in Table 8 show deviations of $0.101 \leq ERD \leq 0.141$, $0.974 \leq EPC \leq 1.118$, and $0.952 \leq SC \leq 0.989$ when compared with the experimental data. All pressure ratio test groups show good agreement with experimental data, with the 5.5 dry simulated case showing the best results.

4.9 Summary

This section presented and discussed the results emanating from the numerical simulation developed in Chapter 3:. The simulated results were compared with the experimental results obtained by Jacobs [53] and showed acceptable agreement. The numerical simulation has thus been validated and can be used to determine the effect that timed coolant injection with suction valve control has on reciprocating compressors.

The following chapter will discuss the comparison between discharge pressure, discharge temperature, and indicated work done per cycle. The application of the model beyond its tested operating range will also be presented.

Chapter 5: Results and discussion

5.1 Introduction

In this chapter, simulated and experimental values of discharge pressure, discharge temperature, and indicated work per cycle will be compared. The application of the model beyond its tested operating range will also be presented.

5.2 Simulated vs experimental results

The simulated discharge pressure for all test groups were compared with the experimental results. Table 9 shows the discharge pressures as well as the error percentage calculated between the experimental and simulated results. It is evident that the higher-pressure-ratio test groups compare better with experimental results with the last simulated case (7 timed coolant injection), rendering a very good result.

Table 10: Simulated vs experimental discharge pressure validation results

Test group	Average experimental discharge pressure (kPa)[a]	Simulated discharge pressure (kPa)	Error percentage (%)
4 Dry	349.5	431.2	23
4 Timed coolant injection	364.6	402.5	10
5.5 Dry	493.2	536.1	9
5.5 Timed coolant injection	489.0	496.7	2
7 Dry	602.2	620.4	3
7 Timed coolant injection	593.0	593.7	0.1

[a] Average experimental discharge pressure calculated from Table 6.2 in [53]

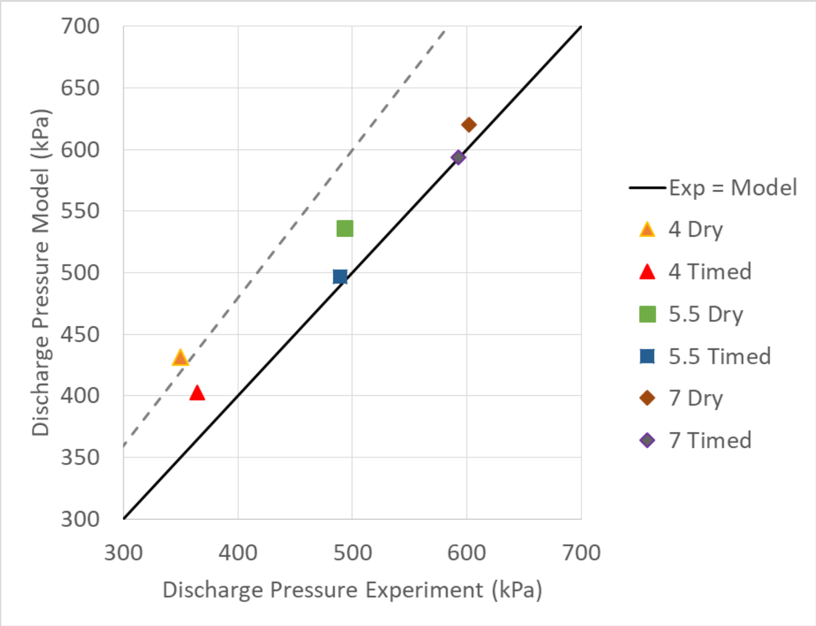

Figure 15: Discharge pressure: Experimental vs simulated results for all cases

The simulated discharge temperature for each timed case was compared with the experimental results. The dry cases were used to determine the heat transfer coefficient calibration factor. Table 10 shows that all timed test groups show good agreement when compared to the experimental results, with the highest error percentage at 6% in the 7 timed coolant injection simulated case. It can be noted that the error percentage rises as the pressure ratio increases.

Table 11: Simulated and experimental discharge temperature comparison

Test group	Average experimental discharge temperature (K) [°C]	Simulated discharge temperature (K) [°C]	Error percentage (%)
4 Timed coolant injection	333.9 [60.7]	344.1 [71.0]	3
5.5 Timed coolant injection	332.2 [59.0]	348.9 [75.8]	5
7 Timed coolant injection	333.7 [60.5]	355 [81.9]	6

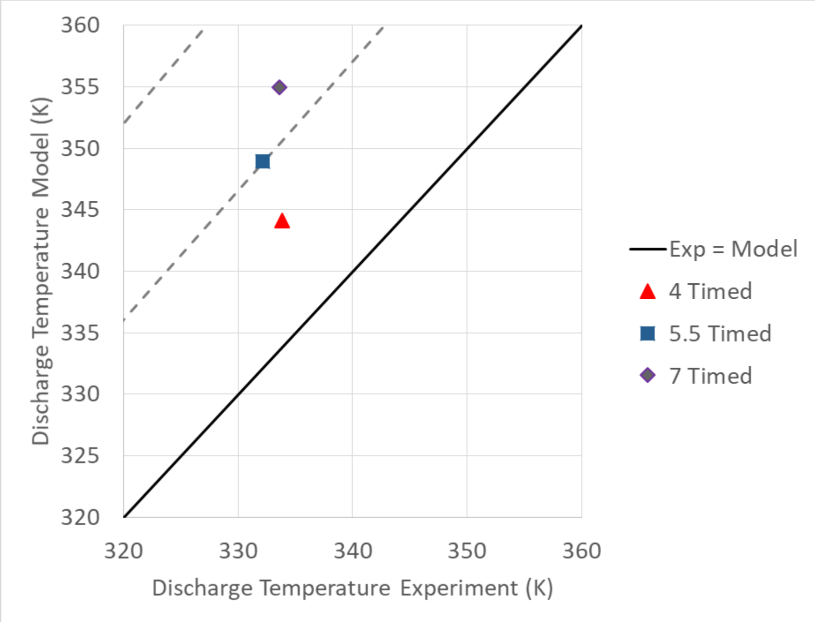

Figure 16: Discharge temperature: Experimental vs simulated results for timed groups

The simulated indicated work per cycle for all test groups were compared with the experimental results. Table 11 shows the indicated work per cycle as well as the error percentage calculated between the experimental and simulated results. The pressure ratio 4 and 7 test groups show good agreement with experimental results, with the 5.5 pressure ratio test group showing the largest disparity.

Table 12: Indicated work done per cycle results

Test group	Average experimental indicated work per cycle (Joule)	Simulated indicated work per cycle (Joule)	Error percentage (%)
4 Dry	29.48	31.33	6
4 Timed coolant injection	27.38	29.53	8
5.5 Dry	32.23	36.07	12
5.5 Timed coolant injection	26.31	32.17	22
7 Dry	33.71	37.53	11
7 Timed coolant injection	32.03	33.65	5

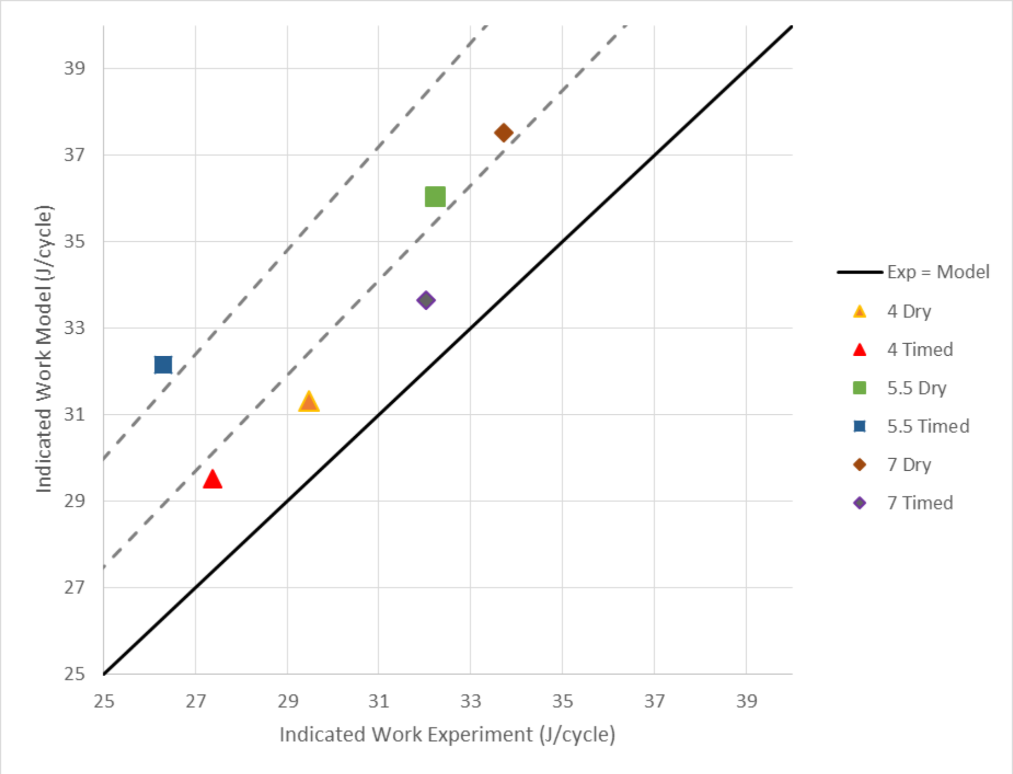

Figure 17: Indicated work per cycle: Experimental vs modelled results for all cases

It is evident in Table 11 that when a comparison between the simulated dry and timed simulated cases are made, the timed simulated case indicates a reduction in work per cycle. This reduction in work signifies the advantage gained when employing valve control with timed coolant injection in reciprocating compressors.

Table 12 shows the reduction in simulated indicated work per cycle for each test group in Joule and as a percentage. It can be seen that the effect of the timed coolant injection with suction valve control increases as the pressure ratio increases. Therefore, an investigation into the application of the model beyond its tested range with a higher pressure ratio will be conducted.

Table 13: Simulated effect of timed coolant injection with suction valve control

Test group	Simulated indicated work per cycle (Joule)	Reduction in simulated indicated work per cycle (Joule)	Percentage saving (%)
4 Dry 4 Timed coolant injection	31.33 29.53	1.8	6
5.5 Dry 5.5 Timed coolant injection	36.07 32.17	3.9	11
7 Dry 7 Timed coolant injection	37.53 33.65	3.9	10

Table 14: Extrapolated input data for the 10 timed test group

Test group	Suction pressure (kPa)	Discharge pressure (kPa)	Suction temperature (˚C)	Discharge temperature (˚C)	Calibration factor (CF_w)	Coolant temperature (˚C)	Pressure ratio	Speed (r/min)	Coolant mass flow rate (kg/s)
10 Dry	87.0	870	44.8	109.6[a]	-	-	10	485.4	0.42×10^{-3}
10 Timed	87.0	870	44.8	60.1	53	10.0	10	485.4	0.42×10^{-3}
10 Timed-Low $T_{coolant}$	87.0	870	44.8	60.1	53	1.0	10	485.4	0.42×10^{-3}
10 Timed-MMF	87.0	870	44.8	60.1	53	1.0	10	485.4	1.27×10^{-3}

[a] Extrapolated from the experimental results presented by Jacobs [53] with *discharge temperature = -0,0073x³ + 0,1532x² + 1,1325x + 90,253,* where x = pressure ratio

5.3 Model application cases

The 4 timed simulation case model was modified to simulate a reciprocating compressor with a pressure ratio of 10:1, as the experimental compressor was designed for this maximum pressure ratio. The input parameters were extrapolated from Table 3 (*cf.* Table 13).

As with the previous cases, the dry simulated case was used to determine the heat transfer coefficient calibration factor. No experimental discharge temperature is available for calibration; therefore, the input discharge temperature was used.

The simulation groups consisted of a dry and timed case that was modified to represent the new pressure ratio. Additionally, a simulation case where the injected coolant temperature was decreased to 1°C (*10 Timed-Low* $T_{coolant}$) and a case where the coolant mass flow rate was increased threefold (*10 Timed-MMF*) were also added.

5.4 Model application cases results discussion

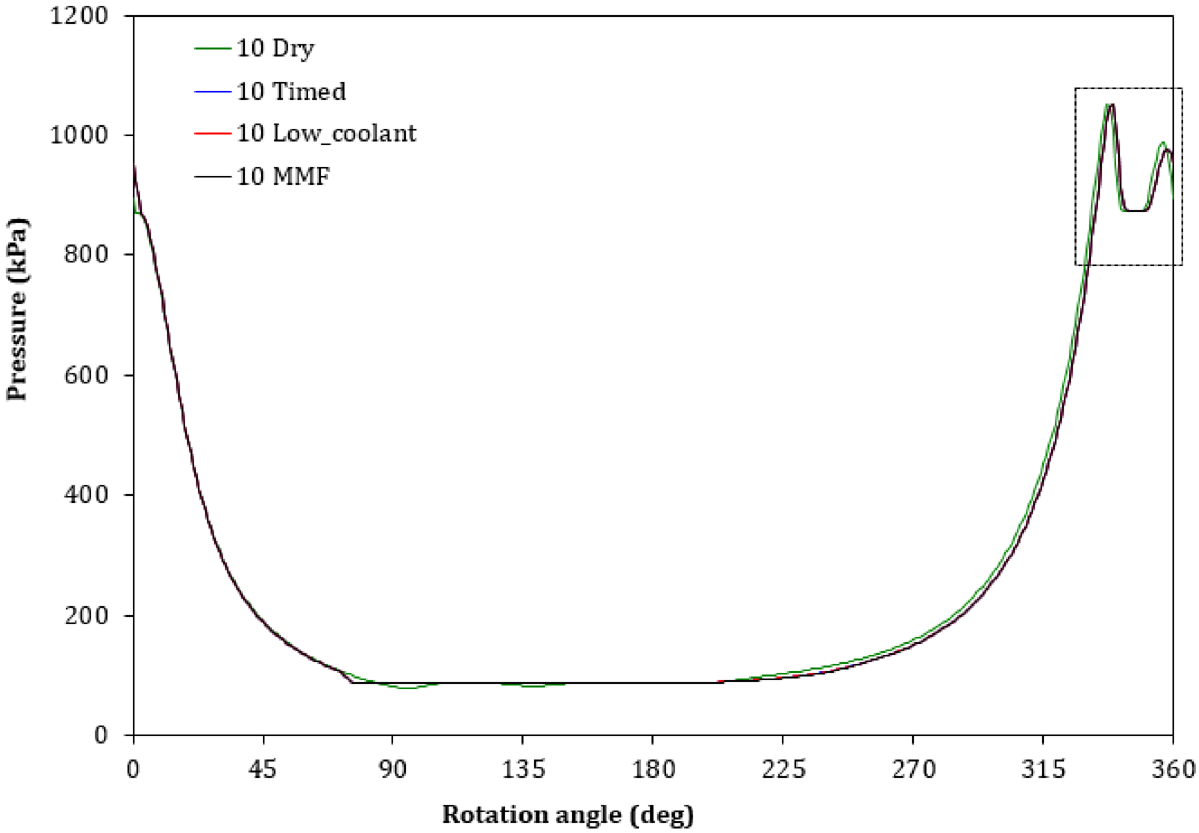

Figure 18: 10:1 Pressure ratio simulated cases: Pressure vs rotational angle data comparison

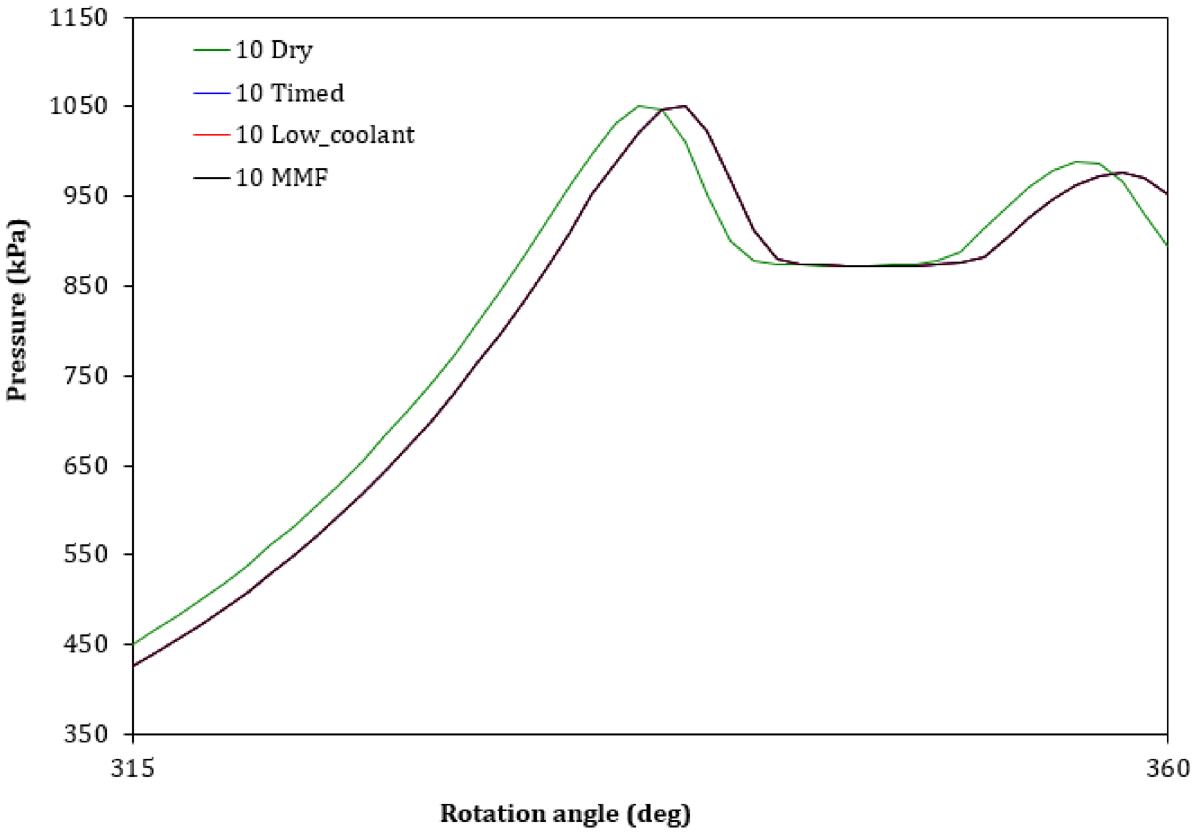

Figure 19: Enlarged area as shown in Figure 18

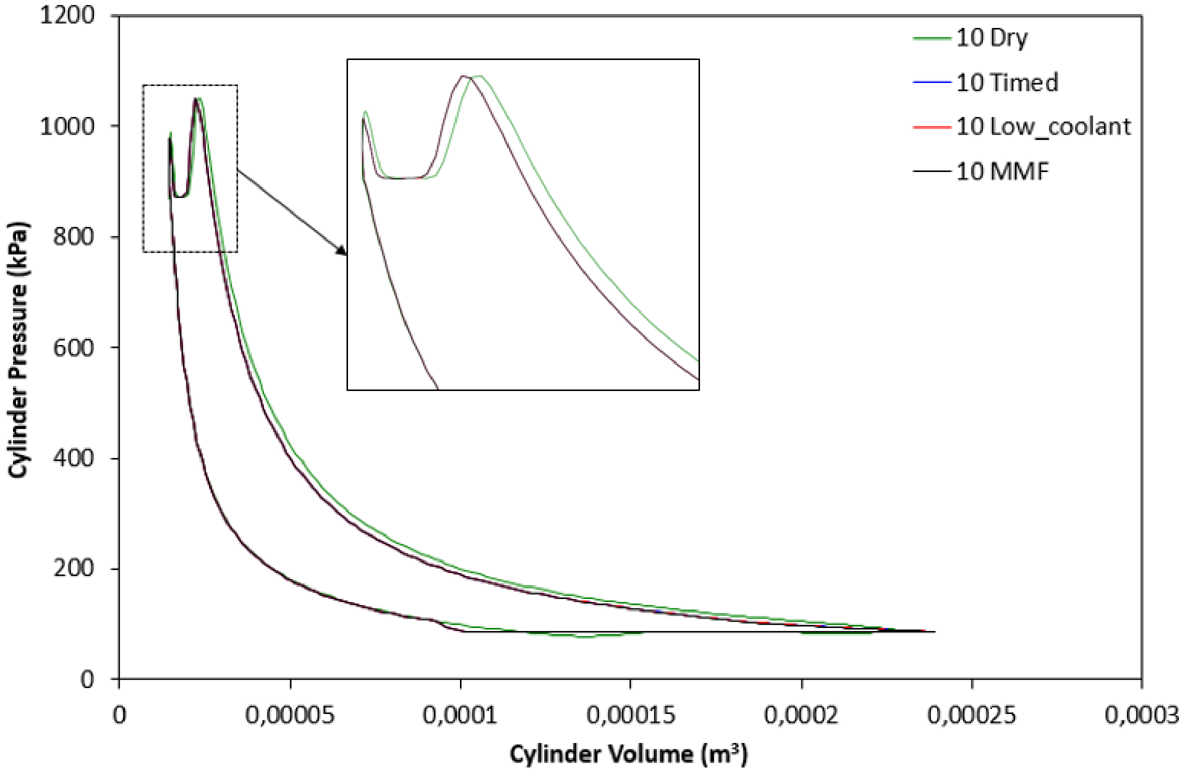

Figure 20: 10:1 Pressure ratio simulated cases: Pressure vs volume data comparison

Table 14 shows the discharge pressure, discharge temperature, and indicated work per cycle. It is evident that the discharge pressure and temperature of the *Timed-Low* $T_{coolant}$ and *Timed-MMF* simulation cases show no deviation from the timed simulation cases.

The indicated work per cycle for the *Timed-Low* $T_{coolant}$ simulated case is similar to the timed simulation case. However, the indicated work per cycle for the *Timed-MMF* simulated case was 0.2% less when compared to the timed and *Timed-Low* $T_{coolant}$.

Table 15: Results of discharge pressure, discharge temperature, and indicated work per cycle for the high-pressure-ratio test group

Test group	Discharge pressure (kPa)	Discharge temperature (K) [˚C]	Simulated indicated work per cycle (Joule)
10 Dry	894.4	-	31.85
10 Timed	952.4	367.67 [94.5]	28.92
10 Timed-Low $T_{coolant}$	952.4	367.67 [94.5]	28.91
10 Timed-MMF	952.4	367.67 [94.5]	28.86

Table 16: Simulated effect of timed coolant injection with suction valve control for all test groups

Test group	Simulated indicated work per cycle (Joule)	Reduction in simulated indicated work per cycle (Joule)	Percentage saving dry vs timed (%)
4 Dry	31.33	1.8	5.7
4 Timed coolant injection	29.53		
5.5 Dry	36.07	3.9	10.8
5.5 Timed coolant injection	32.17		
7 Dry	37.53	3.9	10.3
7 Timed coolant injection	33.65		
10 Dry	31.85	-	-
10 Timed	28.92	2.93	9.2
10 Timed-Low $T_{coolant}$	28.91	2.94	9.2
10 Timed-MMF	28.86	2.99	9.4

Table 15 summarises the simulated indicated work per cycle for each simulation group. When comparing the dry and timed simulation cases, it is evident that the timed cases require less work to be performed to reach the required discharge pressure.

The percentage of work saved increases from 5.7% for the 4 pressure ratio case to 10.3% for the 7 timed case. However, the percentage of work saved starts to decrease as the pressure ratio is increased to 10:1.

Although the percentage of work saved between the dry and timed simulated cases starts to decrease beyond the 5.5 timed test group, the simulated indicated work per cycle of the timed simulated cases for the 10 pressure ratio test group is lower than the 5.5 and 7 timed cases. This indicates a saving of work per cycle, as less work is required to deliver a higher discharge pressure.

5.5 Summary

Chapter 5: compared the simulated and experimental values of discharge pressure, discharge temperature, and indicated work per cycle of the 4, 5.5, and 7 pressure ratio test groups. The application of the model beyond its tested operating range was also presented with the addition of a 10:1 pressure ratio test group. Additional timed scenarios, where the injected coolant temperature was decreased and the coolant mass flow rate was increased, was also presented.

The results from this chapter illustrated that a saving in indicated work could be achieved if valve control with coolant injection is utilised on reciprocating compressors.

Chapter 6: Summary and conclusion

6.1 Introduction

This research study demonstrated the development and validation of a mathematical model, based on the first law of thermodynamics, for a reciprocating compressor subjected to coolant injection and valve control. The simulated data was compared with experimental results and showed overall good agreement.

The validated simulation was used to simulate a pressure ratio beyond its tested operating range. The results of this simulation showed that a saving in indicated work can be achieved at higher pressure ratios.

This chapter will discuss some observations made during modelling, challenges overcame, and recommendations for future research.

6.2 Modelling of a reciprocating compressor with timed coolant injection and valve control

Compressors have broad applications in both the household and industrial sectors. Their application for energy storage schemes such as CAES and CES was discussed in Section 1.1.1, while their energy consumption was investigated in Section 1.1.2.

Pursuant of higher efficiencies, various research studies have been conducted to increase compressor efficiency. These strategies were discussed during the Literature Review conducted in Chapter 2:. The creation of mathematical models, ranging in complexity, to simulate compressors and aid in the design of more efficient compressors was discussed in Section 2.6. The strategy proposed by Jacobs [53] was chosen to create a 1D mathematical model based on the first law of thermodynamics. Chapter 3: described the modelling process and strategy employed to model each subsystem.

6.3 Validation procedure and results

The validation procedure of the simulation, described in Chapter 4:, commenced by initialisation with input data obtained from Jacobs [53]. The input data corresponded with three experimental pressure ratio test cases comprising two test case sets, namely dry and timed. Sections 4.4 to 4.7 described the calibration of the model with experimental data that either was not or could not be measured.

The simulated data obtained was compared with the experimental results in Section 4.8. The Euclidean Relative Difference (ERD), Euclidean Projection Coefficient (EPC), and Secant Cosine (SC) were used to evaluate the error percentage between the experimental and simulated data. These three methods were discussed in Section 4.3.

6.4 Recommended application of the mathematical model

This research study aimed to develop and validate a mathematical model based on the first law of thermodynamics that will support the development of reciprocating compressors with improved efficiency. The current model, with a reduction in indicated work required to achieve high pressure ratios, showed that current reciprocating compressors can be improved

This model can be utilised to design high-pressure-ratio reciprocating compressors that utilise coolant injection and valve control for increased efficiency. These high-pressure-ratio compressors could ideally be used for CAES applications to increase the overall system efficiency.

6.5 Recommendations for future research

This model was created with the intent of forming a foundation for future modelling of a reciprocating compressor with coolant injection and valve control. Thus, keeping the model modular was kept in mind throughout. The model consisted of a main programme with input functions for valves, heat transfer coefficient, etc. These functions can easily be selected, deselected, or replaced by other functions. Additional components not included in the model (*cf.* Figure 9), such as the suction and discharge piping, filters, piston ring leakage, a muffler, etc., should be included and their effect on the overall efficiency accounted for.

The coolant utilised throughout this simulation is water with a temperature ranging from 15°C to 1°C (*cf.* Table 3 & Table 13). Thus, a limiting factor to the effect of the injected coolant is the temperature at which water freezes. The use of heat transfer fluids that can be chilled to below 0°C should be investigated.

The working fluid, air, is assumed to be an ideal gas (*cf.* Equation 19-23) which limits the simulated behaviour of boundary work. This should be explored further.

Although an increase in indicated work has been reported, it should be noted that the increased work required to chill the coolant has not been accounted for. Therefore, the overall efficiency of the system should be investigated.

The current adiabatic mixing process modelled, although suitable for this simulation, could be replaced by a more representative droplet coolant injection model. The effect of coolant evaporation during adiabatic mixing should also be explored.

Future research should include the use of the current model to investigate improvements to coolant injection timing and amount as well as other geometric features. The model could also be used to determine and recommend general compressor improvements. The current model should also be incorporated into a CAES system process model.

6.6 Conclusions

This study showed that when coolant injection and valve control for reciprocating compressors are employed, a reduction in indicated work is achieved.

The model presented here, based on the first law of thermodynamics, was not optimised and included a high calibration factor to simulate the heat transfer through the cylinder walls. Therefore, the current model would benefit from refinement during future research.

Ultimately, this model achieved its aim; that is, to be utilised during the design of efficient compressors and form the basis of more complex and refined models of reciprocating compressors with coolant injection and valve control.

References

[1] T. D. Eastop and A. McConkey, *Applied thermodynamics for engineering technologists*, 5th ed. Pearson Education Limited, 1993.

[2] R. N. Brown, *Compressors: Selection and sizing*. Houston: Gulf Professional, 2005.

[3] E. A. Avallone, T. Baumeister, and L. S. Marks, *Marks' standard handbook for mechanical engineers*. McGraw-Hill, 1996.

[4] W. He and J. Wang, "Optimal selection of air expansion machine in Compressed Air Energy Storage: A review," *Renewable and Sustainable Energy Reviews*, vol. 87, pp. 77–95, May 2018, doi: 10.1016/J.RSER.2018.01.013.

[5] F. Crotogino, K.-U. Mohmeyer, and R. Scharf, "Huntorf CAES: More than 20 Years of Successful Operation," Orlando, Apr. 2001.

[6] B. Elmegaard and W. ; Brix, "Efficiency of Compressed Air Energy Storage," in *The 24th International Conference on Efficiency, Cost, Optimization, Simulation and Environmental Impact of Energy Systems*, 2011.

[7] R. Morgan, S. Nelmes, E. Gibson, and G. Brett, "Liquid air energy storage – analysis and first results from a pilot scale demonstration plant," *Appl Energy*, vol. 137, pp. 845–853, Jan. 2015, doi: 10.1016/J.APENERGY.2014.07.109.

[8] C. Yilmaz, T. H. Cetin, B. Ozturkmen, and M. Kanoglu, "Thermodynamic performance analysis of gas liquefactoin cycles for cryogenic applications," Yildiz Technical University Press, 2019.

[9] P. Krawczyk, Ł. Szabłowski, S. Karellas, E. Kakaras, and K. Badyda, "Comparative thermodynamic analysis of compressed air and liquid air energy storage systems," *Energy*, vol. 142, pp. 46–54, Jan. 2018, doi: 10.1016/J.ENERGY.2017.07.078.

[10] A. Tafone, E. Borri, G. Comodi, M. Van Den Broek, and A. Romagnoli, "Preliminary assessment of waste heat recovery solution (ORC) to enhance the performance of Liquid Air Energy Storage system," in *Energy Procedia*, Elsevier Ltd, 2017, pp. 3609–3616. doi: 10.1016/j.egypro.2017.12.252.

[11] E. Gibson, "Liquid air energy storage (LAES): From pilot plant to multi MW demonstration plant," 2014.

[12] R. Morgan, S. Nelmes, E. Gibson, and G. Brett, "An analysis of a large-scale liquid air energy storage system," *Proceedings of Institution of Civil Engineers: Energy*, vol. 168, no. 2, pp. 135–144, May 2015, doi: 10.1680/ener.14.00038.

[13] Y. Li, H. Chen, X. Zhang, C. Tan, and Y. Ding, "Renewable energy carriers: Hydrogen or liquid air/nitrogen?," *Appl Therm Eng*, vol. 30, no. 14–15, pp. 1985–1990, Oct. 2010, doi: 10.1016/J.APPLTHERMALENG.2010.04.033.

[14] T. Van Nguyen, E. D. Rothuizen, W. B. Markussen, and B. Elmegaard, "Thermodynamic comparison of three small-scale gas liquefaction systems," *Appl Therm Eng*, vol. 128, pp. 712–724, Jan. 2018, doi: 10.1016/J.APPLTHERMALENG.2017.09.055.

[15] C. W. Remeljej and A. F. A. Hoadley, "An exergy analysis of small-scale liquefied natural gas (LNG) liquefaction processes," *Energy*, vol. 31, no. 12, pp. 2005–2019, Sep. 2006, doi: 10.1016/J.ENERGY.2005.09.005.

[16] R. Saidur, N. A. Rahim, and M. Hasanuzzaman, "A review on compressed-air energy use and energy savings," May 2010. doi: 10.1016/j.rser.2009.11.013.

[17] L. Liebenberg, D. Velleman, and W. Booysen, "A simple demand-side management solution for a typical compressed-air system at a South African gold mine," *Journal of Energy in Southern Africa*, vol. 23, no. 2, 2012.

[18] H. Q. Shanghai, A. Mckane, and H. Qin, "Improving Energy Efficiency of Compressed Air System Based on System Audit." [Online]. Available: https://escholarship.org/uc/item/13w7f2fc

[19] J. H. Marais, M. Kleingeld, and R. Pelzer, "Increased energy savings through a compressed air leakage documentation system."

[20] S. Mousavi, S. Kara, and B. Kornfeld, "Energy efficiency of compressed air systems," in *Procedia CIRP*, 2014, pp. 313–318. doi: 10.1016/j.procir.2014.06.026.

[21] F. Ribas, F. Fagotti, T. Dutra, F. A. Ribas Jr, C. J. Deschamps, and A. Morriesen, "Thermal Analysis of Reciprocating Compressors - A Critical Review," 2008. [Online]. Available: https://docs.lib.purdue.edu/icec/1907

[22] J. Huang, S. W. Wang, Y. Luo, Z. C. Zhao, and X. Y. Wen, "Debates on the causes of global warming," *Advances in Climate Change Research*, vol. 3, no. 1, pp. 38–44, 2012, doi: 10.3724/sp.j.1248.2012.00038.

[23] A. Ter-Gazarian, *Energy storage for power systems*. P. Peregrinus on behalf of the Institution of Electrical Engineers, 1994.

[24] Y. A. Cengel and M. A. Boles, *Thermodynamics: An engineering approach*, 7th ed. McGraw-Hill, 2011.

[25] M. W. Coney, P. Stephenson, A. Malmgren, C. Linnemann, and R. E. Morgan, "Development of a reciprocating compressor using water injection to achieve quasi-isothermal compression." [Online]. Available: http://docs.lib.purdue.edu/icec/1508

[26] H. Jouhara, N. Khordehgah, S. Almahmoud, B. Delpech, A. Chauhan, and S. A. Tassou, "Waste heat recovery technologies and applications," *Thermal Science and Engineering Progress*, vol. 6, pp. 268–289, Jun. 2018, doi: 10.1016/J.TSEP.2018.04.017.

[27] J. Wang, J. Wang, P. Zhao, and Y. Dai, "Thermodynamic analysis and comparison study of an Organic Rankine Cycle (ORC) and Kalina cycle for waste heat recovery

of compressor intercooling," 2014. [Online]. Available: https://www.researchgate.net/publication/289004890

[28] S. Murgia, G. Valenti, D. Colletta, I. Costanzo, and G. Contaldi, "Experimental investigation into an ORC-based low-grade energy recovery system equipped with sliding-vane expander using hot oil from an air compressor as thermal source," *Energy Procedia*, vol. 129, pp. 339–346, Sep. 2017, doi: 10.1016/J.EGYPRO.2017.09.204.

[29] S. Shuaihui, Y. Zhao, L. Li, and P. Shu, "Simulation research on scroll refrigeration compressor with external cooling," *International Journal of Refrigeration*, vol. 33, no. 5, pp. 897–906, Aug. 2010, doi: 10.1016/j.ijrefrig.2010.03.005.

[30] X. Wang, Y. Hwang, and R. Radermacher, "Investigation of potential benefits of compressor cooling," *Appl Therm Eng*, vol. 28, no. 14–15, pp. 1791–1797, Oct. 2008, doi: 10.1016/j.applthermaleng.2007.11.010.

[31] A. K. Dutta, T. Yanagisawa, and M. Fukuta, "An investigation of the performance of a scroll compressor under liquid refrigerant injection," *International Journal of Refrigeration*, vol. 24, no. 6, pp. 577–587, Sep. 2001, doi: 10.1016/S0140-7007(00)00041-4.

[32] B. Wang, X. Li, W. Shi, and Q. Yan, "Design of experimental bench and internal pressure measurement of scroll compressor with refrigerant injection," *International Journal of Refrigeration*, vol. 30, no. 1, pp. 179–186, Jan. 2007, doi: 10.1016/J.IJREFRIG.2006.04.007.

[33] H. Sun *et al.*, "A theory-based explicit calculation model for variable speed scroll compressors with vapor injection," *International Journal of Refrigeration*, vol. 88, pp. 402–412, Apr. 2018, doi: 10.1016/J.IJREFRIG.2018.01.016.

[34] I. H. Bell, E. A. Groll, J. E. Braun, G. B. King, and W. T. Horton, "Optimization of a scroll compressor for liquid flooding," *International Journal of Refrigeration*, vol. 35, no. 7, pp. 1901–1913, Nov. 2012, doi: 10.1016/J.IJREFRIG.2012.07.011.

[35] K. Hammerl, L. Rinder, M. Knittl-Frank, and K. Hammerli, "Modifications in the Design of the Oil-Injection System for Screw Compressors," 2000. [Online]. Available: http://docs.lib.purdue.edu/icec/1489

[36] M. De Paepe, W. Bogaert, and D. Mertens, "Cooling of oil injected screw compressors by oil atomisation," *Appl Therm Eng*, vol. 25, no. 17–18, pp. 2764–2779, Dec. 2005, doi: 10.1016/J.APPLTHERMALENG.2005.02.003.

[37] D. P. Georgiou and T. Xenos, "The process of isothermal compression of gasses at sub-atmospheric pressures through regulated water injection in Braysson cycles," *Appl Therm Eng*, vol. 31, no. 14–15, pp. 2205–2212, Oct. 2011, doi: 10.1016/J.APPLTHERMALENG.2010.11.033.

[38] S. Jarungthammachote, "Optimal interstage pressures of multistage compression with intercooling processes," *Thermal Science and Engineering Progress*, vol. 29, p. 101202, Mar. 2022, doi: 10.1016/J.TSEP.2022.101202.

[39] C. Subramaniyan, B. Kalidasan, N. Bhuvanesh, K. B. Prakash, and A. Amarkarthik, "Second law analysis on performance of double stage reciprocating air compressor with inter cooler," *Mater Today Proc*, vol. 45, pp. 652–657, Jan. 2021, doi: 10.1016/J.MATPR.2020.02.727.

[40] Y. Liu, N. Miao, Y. Deng, and D. Wu, "Efficiency evaluation of a miniature multi-stage compressor under insufficient inter-stage cooling conditions," *International Journal of Refrigeration*, vol. 97, pp. 169–179, Jan. 2019, doi: 10.1016/J.IJREFRIG.2018.09.009.

[41] M. Heidari, S. Lemofouet, and A. Rufer, "On the strategies towards isothermal gas compression and expansion." [Online]. Available: http://docs.lib.purdue.edu/icec/2285

[42] M. Heidari, M. Mortazavi, and A. Rufer, "Design, modeling and experimental validation of a novel finned reciprocating compressor for Isothermal Compressed Air Energy Storage applications," *Energy*, vol. 140, pp. 1252–1266, Dec. 2017, doi: 10.1016/J.ENERGY.2017.09.031.

[43] C. Knowlen, J. Williams, A. T. Mattick, H. Deparis, and A. Hertzberg, "Quasi-Isothermal Expansion Engines for Liquid Nitrogen Automotive Propulsion," 1997.

[44] J. D. Van de Ven and P. Y. Li, "Liquid piston gas compression," *Appl Energy*, vol. 86, no. 10, pp. 2183–2191, Oct. 2009, doi: 10.1016/J.APENERGY.2008.12.001.

[45] C. Qin and E. Loth, "Liquid piston compression efficiency with droplet heat transfer," *Appl Energy*, vol. 114, pp. 539–550, Feb. 2014, doi: 10.1016/J.APENERGY.2013.10.005.

[46] V. E. Shcherba, E. A. Pavlyuchenko, E. Y. Nosov, and I. Yu Bulgakova, "Approximation of the compression process to isothermal in a reciprocating compressor with a liquid piston," *Appl Therm Eng*, vol. 207, p. 118151, May 2022, doi: 10.1016/J.APPLTHERMALENG.2022.118151.

[47] I. H. Bell, E. A. Groll, and J. E. Braun, "Performance of vapor compression systems with compressor oil flooding and regeneration," *International Journal of Refrigeration*, vol. 34, no. 1, pp. 225–233, Jan. 2011, doi: 10.1016/J.IJREFRIG.2010.09.004.

[48] X. Xu, Y. Hwang, and R. Radermacher, "Refrigerant injection for heat pumping/air conditioning systems: Literature review and challenges discussions," *International Journal of Refrigeration*, vol. 34, no. 2, pp. 402–415, Mar. 2011, doi: 10.1016/J.IJREFRIG.2010.09.015.

[49] R. Kremer, C. J. Deschamps, and J. R. Barbosa, "Theoretical analysis of the effect of oil atomization in the cylinder of a reciprocating ammonia compressor," 2008. [Online]. Available: http://docs.lib.purdue.edu/icec/1909

[50] R. Kremer, C. J. Deschamps, and J. R. Barbosa, "Cooling of a reciprocating compressor through oil atomization in the cylinder," 2010. [Online]. Available: http://docs.lib.purdue.edu/icec/1986

[51] M. Malmgren, J. Sidders, P. Stephenson, and M. Coney, "Experiments and simulations of a quasi-isothermal compressor for a novel high efficiency engine," *International conference on compressors and their systems*, pp. 461–470, Sep. 2003.

[52] G. G. Jacobs and L. Liebenberg, "The influence of timed coolant injection on compressor efficiency," *Sustainable Energy Technologies and Assessments*, vol. 18, pp. 175–189, Dec. 2016, doi: 10.1016/J.SETA.2016.10.010.

[53] G. G. Jacobs, "The influence of controlled coolant injection on quasi-isothermal compression," PhD thesis, North-West University, Potchefstroom, South Africa, 2014.

[54] W. J. D. Annand, "Heat Transfer in the Cylinders of Reciprocating Internal Combustion Engines," *Proceedings of the Institution of Mechanical Engineers*, vol. 177, no. 1, pp. 973–996, Jun. 1963, doi: 10.1243/PIME_PROC_1963_177_069_02.

[55] G. Woschni, "A universally applicable equation for the instantaneous heat transfer coefficient in the internal combustion engine," *Society of Automotive Engineers*, p. 3065, 1967.

[56] R. P. Adair, E. B. Qvale, and J. T. Pearson, "Instantaneous Heat Transfer to the Cylinder Wall in Reciprocating Compressors." [Online]. Available: http://docs.lib.purdue.edu/icec/86

[57] F. Fagotti, M. L. Todescat, R. T. S. Ferreira, and A. T. Prata, "Heat Transfer Modeling in a Reciprocating compressor." [Online]. Available: http://docs.lib.purdue.edu/icec/1043

[58] F. Fagotti and A. . T. Prata, "A new correlation for instantaneous heat transfer between gas and cylinder in reciprocating compressors." [Online]. Available: http://docs.lib.purdue.edu/icec/1351

[59] F. P. Disconzi, C. J. Deschamps, and E. L. L. Pereira, "Development of an In-Cylinder Heat Transfer Correlation for Reciprocating Compressors." [Online]. Available: https://docs.lib.purdue.edu/icec

[60] J. Tuhovcak, J. Hejcik, and M. Jicha, "Comparison of heat transfer models for reciprocating compressor," *Appl Therm Eng*, vol. 103, pp. 607–615, Jun. 2016, doi: 10.1016/j.applthermaleng.2016.04.120.

[61] J. Tuhovcák, í Hej, M. Jícha, J. Tuhovcak, J. Hejcik, and M. Jicha, "Heat Transfer Analysis in the Cylinder of Reciprocating Compressor," 2016. [Online]. Available: https://docs.lib.purdue.edu/icec

[62] H. Bukac, "Understanding Valve Dynamics." [Online]. Available: https://docs.lib.purdue.edu/icec

[63] D. Taranović, S. Milojević, and R. Pesic, "Modelling valve dynamics and flow in reciprocating compressors," 2013. [Online]. Available: https://www.researchgate.net/publication/323560736

[64] M. Volf and P. Eret, "A study of reciprocating compressor valve dynamics," 2016.

[65] R. A. Habing, "Flow and plate motion in compressor valves," 2005.

[66] R. A. Habing and M. C. A. M. Peters, "An experimental method for validating compressor valve vibration theory," *J Fluids Struct*, vol. 22, no. 5, pp. 683–697, Jul. 2006, doi: 10.1016/j.jfluidstructs.2006.03.003.

[67] J. Tuhovcak, J. Hejčík, and M. Jícha, "Modelling fluid flow in a reciprocating compressor," in *EPJ Web of Conferences*, EDP Sciences, May 2015. doi: 10.1051/epjconf/20159202100.

[68] M. M. Tanveer, C. R. Bradshaw, X. Ding, and D. Ziviani, "Mechanistic chamber models: A review of geometry, mass flow, valve, and heat transfer sub-models," *International Journal of Refrigeration*, vol. 142, pp. 111–126, Oct. 2022, doi: 10.1016/j.ijrefrig.2022.06.016.

[69] L. Boswirth, "Non Steady Flow in Valves," 1990. [Online]. Available: http://docs.lib.purdue.edu/icec/759

[70] M. N. Srinivas and C. Padmanabhan, "Computationally efficient model for refrigeration compressor gas dynamics," *International Journal of Refrigeration*, vol. 25, no. 8, pp. 1083–1092, Dec. 2002, doi: 10.1016/S0140-7007(01)00109-8.

[71] R. Singh and W. Soedel, "Mathematical modeling of multicylinder compressor discharge system interactions," *J Sound Vib*, vol. 63, no. 1, pp. 125–143, 1979.

[72] W. Soedel, *Introduction to computer simulation of positive displacement compressors*. 1972.

[73] B. D. Rasmussen and A. Jakobsen, "Review of Compressor Models and Performance Characterizing Variables," 2000. [Online]. Available: https://docs.lib.purdue.edu/icec

[74] M. E. Duprez, E. Dumont, and M. Frère, "Modelling of reciprocating and scroll compressors," *International Journal of Refrigeration*, vol. 30, no. 5, pp. 873–886, Aug. 2007, doi: 10.1016/J.IJREFRIG.2006.11.014.

[75] E. Winandy, C. Saavedra O, and J. Lebrun, "Simplified modelling of an open-type reciprocating compressor," *International Journal of Thermal Sciences*, vol. 41, no. 2, pp. 183–192, Feb. 2002, doi: 10.1016/S1290-0729(01)01296-0.

[76] C. O. R. Negrão, R. H. Erthal, D. E. V. Andrade, and L. W. Da Silva, "A semi-empirical model for the unsteady-state simulation of reciprocating compressors for household refrigeration applications," *Appl Therm Eng*, vol. 31, no. 6–7, pp. 1114–1124, May 2011, doi: 10.1016/J.APPLTHERMALENG.2010.12.006.

[77] C. R. Bradshaw, E. A. Groll, and S. V Garimella, "A Comprehensive Model of a Miniature-Scale Linear Compressor for Electronics Cooling," 2010. [Online]. Available: https://docs.lib.purdue.edu/icec

[78] O. Yang, P. Engel, B. G. Shiva, P. Dresser, and R. D. Woollatt, "Dynamic Response of Compressor Valve Springs to Impact Loading," 1996. [Online]. Available: https://docs.lib.purdue.edu/icec

[79] L. Boswirth, "Theoretical and Experimental Study on Valve Flutter T," in *International Compressor Engineering Conference*, 1990. [Online]. Available: https://docs.lib.purdue.edu/icec

[80] R. Dufour, J. Der Hagopian, and M. Lalane, "TRANSIENT AND STEADY STATE DYNAMIC BEHAVIOUR OF SINGLE CYLINDER COMPRESSORS: PREDICTION AND EXPERIMENTS," 1995.

[81] P. Haberschill, M. Laflemand, S. Borg, and M. Mondot, "Hermetic compressor models determination of parameters from a minimum number of tests." [Online]. Available: https://docs.lib.purdue.edu/icec

[82] J. Tuhovþák, J. Hejþík, M. Jícha, and L. Šnajdárek, "Experimental validation of mathematical model for small air compressor."

[83] S. Lee, R. Singh, and M. J. Moran, "First Law Analysis of a Compressor Using a Computer Simulation Model," 1982. [Online]. Available: https://docs.lib.purdue.edu/icec

[84] M. Mohammadi-Amin, A. R. Jahangiri, and M. Bustanchy, "Thermodynamic modeling, CFD analysis and parametric study of a near-isothermal reciprocating compressor," *Thermal Science and Engineering Progress*, vol. 19, p. 100624, Oct. 2020, doi: 10.1016/J.TSEP.2020.100624.

[85] R. Aigner and H. Steinrück, "Modelling Fluid Dynamics, Heat Transfer and Valve Dynamics in a Reciprocating Compressor EFRC RESEARCH."

[86] F. Balduzzi, A. Tanganelli, G. Ferrara, and A. Babbini, "Two-dimensional approach for the numerical simulation of large bore reciprocating compressors thermodynamic cycle," *Appl Therm Eng*, vol. 129, pp. 490–501, Jan. 2018, doi: 10.1016/J.APPLTHERMALENG.2017.10.041.

[87] W. Lang, R. Almbauer, A. Burgstaller, and D. Nagy, "Coupling of 0-,1-and 3-d tool for the simulation of the suction line of a hermetic reciprocating compressor." [Online]. Available: https://docs.lib.purdue.edu/icec

[88] K. Suh, D. Heo, and H. Kim, "CAE/CFD application for linear compressor." [Online]. Available: https://docs.lib.purdue.edu/icec

[89] E. L. L. Pereira, C. J. Santos, C. J. Deschamps, and R. Kremer, "A Simplified Computational Fluid Dynamics Model for the Suction Process of Reciprocating Compressors." [Online]. Available: https://docs.lib.purdue.edu/icec

[90] J. F. Lacerda and C. K. Takemori, "CFD approach to evaluate heat transfer in reciprocating compressors." [Online]. Available: https://docs.lib.purdue.edu/icec

[91] R. Eettisseri, M. Real, and S. Oliveira, "Analysis Of Dynamic Heat Transfer Coefficient In a Reciprocating Compressor By Immersed Solid Method in CFD," 2021. [Online]. Available: https://docs.lib.purdue.edu/icec

[92] E. L. L. Pereira, C. J. Deschamps, and F. A. Ribas, "A Comparative Analysis of Numerical Simulation Approaches for Reciprocating Compressors," 2008. [Online]. Available: https://docs.lib.purdue.edu/icec

[93] R. Kremer, J. R. Barbosa, and C. J. Deschamps, "Cooling of a reciprocating compressor through oil atomization in the cylinder," 2012, doi: 10.1080/10789669.2012.646571.

[94] P. J. Singh and G. C. Patel, "A Generalized Performance Computer Program for Oil Flooded Twin-Screw Compressors," 1984. [Online]. Available: https://docs.lib.purdue.edu/icec

[95] A. Khan and C. R. Bradshaw, "Quantitative Comparison of the Performance of Vapor Compression Cycles with Various Means of Compressor Flooding," 2022. [Online]. Available: https://docs.lib.purdue.edu/icec

[96] S. Höhne, M. L. Taboada, J. Schröder, C. Gomez, H. P. Karbstein, and V. Gaukel, "Influence of Nozzle Geometry and Scale-Up on Oil Droplet Breakup in the Atomization Step during Spray Drying of Emulsions," *Fluids*, vol. 9, no. 3, Mar. 2024, doi: 10.3390/fluids9030070.

Central University of Technology, Free State

Appendix A

Program Listing: First law of thermodynamics model

DYNAMIC SIMULATION OF RECIPROCATING COMPRESSOR USING THE ENERGY EQUATION
(Unit system: kg, m, sec, Joule, Kelvin,rad)

Compressor inputs:

$N := 489.1$ Compressor speed (r/min)

$\omega := \frac{2 \cdot \pi \cdot N}{60}$ $\omega = 51.218432229$ Compressor angular velocity

$L_{str} := 0.060$ Stroke length (Lombardini 15 LD 225)

$L_{con} := 0.1$ Connecting rod length (Lombardini 15 LD 225)

$D_{cyl} := 0.069$ Cylinder diameter

$A_{cyl} := \frac{\pi}{4} \cdot D_{cyl}^{2}$ $A_{cyl} = 0.003739281$ Cylinder cross sectional area

$V_{str} := A_{cyl} \cdot L_{str}$ $V_{str} = 0.000224357$ Stroke volume

$R := 287$ Specific gas constant of Air

$\gamma := 1.4$ Ratio of specific heats

$C_p := 1005$

$C_v := 718$ Specific heats

$Clearance := 6.56\%$ Percentage clearance volume

$V_{cle.dry} := Clearance \cdot V_{str}$ $V_{cle.dry} = 0.000014718$ Dry clearance volume

$FracCleVol := 0$ Fraction of clearance volume occupied by coolant build-up. Range from 0 (dry) to 1 (completely filled)

$V_{cle} := (1 - FracCleVol) \cdot V_{cle.dry}$ Effective clearance volume

$h_{cle} := 0.0005$ Clearance height between piston & cylinder top

<u>Compressor initial inputs:</u>

$P_s := 87 \cdot 10^3$		Suction pressure
$P_d := 364.6 \cdot 10^3$		Discharge pressure
$P_{ratio} := \dfrac{P_d}{P_s}$	$P_{ratio} = 4.190804598$	Pressure ratio
$T_s := 273.15 + 44.8$	$T_s = 317.95$	Suction temperature
$T_d := 273.15 + 60.7$	$T_d = 333.85$	
$T_w := \dfrac{(T_s + T_d)}{2}$	$T_w - 273.15 = 52.75$	Cylinder wall temperature
$T_{cool} := 273.15 + 15.3$	$T_{cool} = 288.45$	Coolant temperature
$\rho_s := \dfrac{P_s}{R \cdot T_s}$	$\rho_s = 0.953407418$	Density of Air at suction
$\rho_d := \dfrac{P_d}{R \cdot T_d}$	$\rho_d = 3.805251686$	Initial estimate of density of Air at discharge

Properties of Water

Correlations for the liquid water thermophysical properties internal energy (u), isochoric specific heat capacity (Cv), isobaric specific heat capacity (Cp) and density (ρ) were derived by means of curve fits from Engineering Equation Solver (EES) produced properties for water. EES makes use of Hyland and Wexler, Formulations for the Thermodynamic Properties of the Saturated Phases of H2O from 173.15 K to 473.15 K, ASHRAE Trans., Part 2A, Paper 2793, 1983. to determine the thermophysical properties of water. The above properties for water are dependant temperature. Pressure has a negligible influence in the pressure range considered i.e. 100 kPa to 10 000 kPa. The correlations are only valid for temperatures between 274 K and 360 K (1°C - 87°C).

u=(-1142.46138 + 4.18289939*T)*1000 (J/kg)

cv=(3.82779518 + 0.0058718703*T1 - 0.0000162788155*T1^2)*1000 (J/kg.K)

cp=(5.74494886 - 0.00985993986*T1 + 0.0000154948162*T1^2)*1000 (J/kg.K)

cv=(3827.79518 + 5.8718703*T1 - 0.0162788155*T1^2) (J/kg.K)

cp=(5744.94886 - 9.85993986*T1 + 0.0154948162*T1^2) (J/kg.K)

$$u_w(T) := (-1142.46138 + 4.18289939 \cdot T) \cdot 1000$$

$$Cp_w(T) := 5744.94886 - 9.85993986 \cdot T + 0.0154948162 \cdot T^2$$

$$Cv_w(T) := 3827.79518 + 5.8718703 \cdot T - 0.0162788155 \cdot T^2$$

$$\rho_w(T) := (165.845153) + 7.43367357 \cdot T - 0.0209620692 \cdot T^2 + 0.0000180593304 \cdot T^3$$

$P = 1000\ kPa$
$274\ K \le T \le 360\ K$

$u_w(280) = 28750.4492$ $\qquad u_{cool}(T) := u_w(T)$

$Cp_w(280) = 4198.95928928$ $\qquad Cp_{cool}(T) := Cp_w(T)$

$Cv_w(280) = 4195.6597288$ $\qquad Cv_{cool}(T) := Cv_w(T)$

$\rho_w(274) = 1000.418711137$ $\qquad \rho_{cool}(T) := \rho_w(T)$

Assign coolant properties to water properties.
Other coolants can be used without affecting the main program syntax.

<u>Coolant mass flow options:</u>

$C_d := 0.3$ — Coolant injector coefficient of discharge

$P_{inj} := 5 \cdot 10^6$ — Coolant injection pressure, see Jacobs Thesis

$\rho_{water} := 998$ — Density of water

$d_{nozzle} := 0.0003$ — Diamter of nozzle, see Jacobs Thesis

$$Q := C_d \cdot \left(\frac{\pi}{4} \cdot d_{nozzle}^{\ 2}\right) \cdot \sqrt{\frac{(2 \cdot P_{inj})}{\rho_{water}}}$$

$m'_{coolant} := Q \cdot \rho_{water}$ $\qquad m'_{coolant} = 0.002118453$

Define adiabatic mixing effectiveness factor: $\varepsilon := 0.2$

$m'_{coolant\_frac} := 1$ — Coolant fraction of total mass flow rate

$m'_{cool} := \varepsilon \cdot m'_{coolant} \cdot m'_{coolant\_frac}$ Coolant mass flow rate

$m'_{cool} = 0.000423691$

Note:
Alternative to the methodology above the coolant mass flow rate could be directly specified with $m'_{cool} =$

$FracCleVol = 0$ Fraction of clearance volume filled by coolant.

$V_{cle.dry} = 0.000014718$

$V_{cool.cle} := FracCleVol \cdot V_{cle.dry}$

$m_{cool.cle} := \rho_{cool}\left(T_{cool}\right) \cdot V_{cool.cle} = 0$ Mass of coolant in clearance volume.

Program inputs:

$no\_divs := 50000$ Number of divisions per revolution

$Number\_of\_revs := 6$ Number of revolutions

Valve and cooling timing:

Automatic plate valves:	valves = 0
Simple check valves:	valves = 1
Timed valves:	valves = 2
Timed valves + cooling:	valves = 3
Timed suction valve + discharge automatic valve + cooling:	valves = 4
No valves (for verification purposes)	valves = 99

$valves := 4$

Check valve with plate valve properties:	chkv_ideal = 0
Ideal check valve with no losses:	chkv_ideal = 1

$chkv\_ideal := 0$

$\theta_{so} := 90 \cdot deg$ Suction valve open angle - Timed

$\theta_{sc} := 195 \cdot deg$ Suction valve close angle - Timed

$\theta_{so.c} := 70 \cdot deg$ Suction valve open angle -Timed + cooling

$\theta_{sc.c} := 174.8 \cdot deg$ Suction valve close angle - Timed + cooling

$\theta_{do} := 315 \cdot deg$ Discharge valve open angle - Timed

$\theta_{dc} := 359 \cdot deg$ Discharge valve close angle - Timed

$\theta_{do.c} := 327 \cdot deg$ Discharge valve open angle - Timed + cooling

$\theta_{dc.c} := 355 \cdot deg$ Discharge valve close angle - Timed + cooling

$\theta_{s\_cool} := 180 \cdot deg$ Cooling timing angle - start cooling

$\theta_{e\_cool} := 240 \cdot deg$ Cooling timing angle - end cooling

Piston motion:

$$n_{ratio} := \frac{L_{con}}{\frac{L_{str}}{2}} = 3.333333333$$

Displacement $$s_{shm}(t) := \left| \frac{L_{str}}{2} \cdot (1 - \cos(\omega \cdot t)) + L_{con} \cdot \frac{(\sin(\omega \cdot t))^2}{2 \cdot (n_{ratio})^2} \right|$$

Piston Velocity $$v_{shm}(t) := \left| \omega \cdot \frac{L_{str}}{2} \cdot \left(\sin(\omega \cdot t) + \frac{\sin(2 \cdot (\omega \cdot t))}{2 \cdot n_{ratio}} \right) \right|$$

Valve data:

$m_{sv} := 0.026$ Mass (kg) of suction valve

$m_{dv} := 0.026$ Mass (kg) of discharge valve

$D_{sv} := 0.0286$ Valve cross sectional flow diameter

$D_{dv} := 0.016$

$r_{sv} := 0.5 \cdot D_{sv}$ $r_{sv} = 0.0143$

Valve cross sectional flow radius

$r_{dv} := 0.5 \cdot D_{dv}$ $r_{dv} = 0.008$

$A_{sv} := \frac{\pi}{4} \cdot D_{sv}^{2}$ $A_{sv} = 0.000642424$

Valve cross sectional flow areas

$A_{dv} := \frac{\pi}{4} \cdot D_{dv}^{2}$ $A_{dv} = 0.000201062$

$max\_position_{sv} := 0.0059$ Maximum valve displacement

$max\_position_{dv} := 0.0097$

$x\_max := max\_position_{dv}$

$y\_max := max\_position_{sv}$

$x_{timed} := x\_max$

Valve lift height if timed

$y_{timed} := y\_max$

$k_s := 1946$ Suction valve spring stiffness (N/m)

$k_d := 1946$ Discharge valve spring stiffness (N/m)

$F_{preload} := 16.53$ Pre-load on discharge valve spring (N)

$c_{damping} := 0.5$ Damping coefficient (N.s/m)

$C_{fs} := 1$

Valve coefficient that accounts for loss of energy due to orifice flow entrance friction effects are ignored if Cf = 1

$C_{fd} := 1$

$D_s := 0.0286$

Valve diameter on which pressure acts

$D_d := 0.016$

$A_s := \frac{\pi}{4} \cdot D_s^{2}$ $A_s = 0.000642424$ Valve area on which pressure acts

$A_d := \frac{\pi}{4} \cdot D_d^{2}$ $\quad A_d = 0.000201062$

$af := 0.2$

Adjustment factor for valve Cd function

$$Cd(x, d) := \frac{0.2}{\frac{x}{d} + 0.29} + 0.32 - af$$

Valve coefficient of discharge function

$C_{ds} := 0.625$

$C_{dd} := 0.625$

Valve coefficients of discharge for use with Simple Check valves

$\theta_{rise} := 22.65 \cdot deg$

$\theta_{fall} := \theta_{rise}$

Suction valve rise and fall angles

```
valve_opt_suc := | if valves = 0
                 |   | option ← "Automatic plate valve"
                 | if valves = 1
                 |   | option ← "Simple check valve"
                 | if valves = 2
                 |   | option ← "Timed valve"
                 | if valves = 3
                 |   | option ← "Timed valve + cooling"
                 | if valves = 4
                 |   | option ← "Timed valve"
                 | if valves = 99
                 |   | option ← "No valve"
                 | option
```

$$valve\_opt\_dis := \begin{array}{|l} \text{if } valves = 0 \\ \quad option \leftarrow \text{"Automatic plate valve"} \\ \text{if } valves = 1 \\ \quad option \leftarrow \text{"Simple check valve"} \\ \text{if } valves = 2 \\ \quad option \leftarrow \text{"Timed valve"} \\ \text{if } valves = 3 \\ \quad option \leftarrow \text{"Timed valve + cooling"} \\ \text{if } valves = 4 \\ \quad option \leftarrow \text{"Automatic plate valve"} \\ \text{if } valves = 99 \\ \quad option \leftarrow \text{"No valve"} \\ option \end{array}$$

$$s\_valve\_open\_angle := \begin{array}{|l} \text{if } valves = 3 \\ \quad svstartang \leftarrow \dfrac{\theta_{so.c}}{deg} \\ \text{if } valves = 4 \\ \quad svstartang \leftarrow \dfrac{\theta_{so.c}}{deg} \\ svstartang \end{array}$$

$$s\_valve\_close\_angle := \begin{array}{|l} \text{if } valves = 3 \\ \quad svcloseang \leftarrow \dfrac{\theta_{sc.c}}{deg} \\ \text{if } valves = 4 \\ \quad svcloseang \leftarrow \dfrac{\theta_{sc.c}}{deg} \\ svcloseang \end{array}$$

$$cool\_start\_angle := \begin{array}{|l} \text{if } valves = 3 \\ \quad coolstartang \leftarrow \dfrac{\theta_{s\_cool}}{deg} \\ \text{if } valves = 4 \\ \quad coolstartang \leftarrow \dfrac{\theta_{s\_cool}}{deg} \\ coolstartang \end{array}$$

$$cool\_end\_angle := \left\| \begin{array}{l} \text{if } valves = 3 \\ \quad \left\| \; coolendang \leftarrow \dfrac{\theta_{e\_cool}}{deg} \right. \\ \text{if } valves = 4 \\ \quad \left\| \; coolendang \leftarrow \dfrac{\theta_{e\_cool}}{deg} \right. \\ coolendang \end{array} \right.$$

$$Valve\_data := \begin{bmatrix} \text{"VARIABLE"} & \text{"(UNITS)"} & \text{"SUCTION"} & \text{"DISCHARGE"} \\ \text{"Plate mass"} & \text{"(kg)"} & m_{sv} & m_{dv} \\ \text{"Discharge coeff."} & \text{"n/a"} & \text{"Cd(x,d)"} & \text{"Cd(x,d)"} \\ \text{"Crossect. flow diam."} & \text{"(m)"} & D_{sv} & D_{dv} \\ \text{"Max. valve displ."} & \text{"(m)"} & max\_position_{sv} & max\_position_{dv} \\ \text{"Valve lift height (timed)"} & \text{"(m)"} & y_{timed} & x_{timed} \\ \text{"Orifice flow loss coeff."} & \text{"n/a"} & C_{fs} & C_{fd} \\ \text{"Valve spring stiffness"} & \text{"(N/m)"} & k_s & k_d \\ \text{"Valve damping coefficient"} & \text{"(N.s/m)"} & c_{damping} & c_{damping} \\ \text{"Valve pressure diam."} & \text{"(m)"} & D_s & D_d \\ \text{"Valve option"} & \text{"n/a"} & valve\_opt\_suc & valve\_opt\_dis \\ \text{"START \& END ANGLES"} & \text{""} & \text{"START ANGLE"} & \text{"END ANGLE"} \\ \text{"Suction valve"} & \text{"(deg)"} & s\_valve\_open\_angle & s\_valve\_close\_angle \\ \text{"Cooling"} & \text{"(deg)"} & cool\_start\_angle & cool\_end\_angle \end{bmatrix}$$

$$chkv\_ideal\_properties := \left\| \begin{array}{l} \text{if } chkv\_ideal = 1 \\ \quad \left\| \begin{array}{l} d_{sv} \leftarrow D_{sv} \cdot 2 \\ d_{dv} \leftarrow D_{dv} \cdot 2 \\ c_{ds} \leftarrow 1 \\ c_{dd} \leftarrow 1 \end{array} \right. \\ \text{if } chkv\_ideal = 0 \\ \quad \left\| \begin{array}{l} d_{sv} \leftarrow D_{sv} \\ d_{dv} \leftarrow D_{dv} \\ c_{ds} \leftarrow C_{ds} \\ c_{dd} \leftarrow C_{dd} \end{array} \right. \\ \text{augment}\left(d_{sv}, d_{dv}, c_{ds}, c_{dd}\right) \end{array} \right.$$

$$D_{sv} := chkv\_ideal\_properties_{0,0}$$

$$D_{dv} := chkv\_ideal\_properties_{0,1}$$

$$C_{ds} := chkv\_ideal\_properties_{0,2}$$

$$C_{dd} := chkv\_ideal\_properties_{0,3}$$

$$k_{air}(T) := \left| \begin{array}{l} \text{"Thermal conductivity (W/m.K) for air - ideal gas (temps = Kelvin)"} \\ \text{"Valid between 143 \& 1050 Kelvin"} \\ \text{if } 143 \le T < 1050 \\ \quad \left\| \begin{array}{l} \text{""} \\ k \leftarrow 1.64301699 \cdot 10^{-3} + 8.60224688 \cdot 10^{-5} \cdot T - 2.06562347 \cdot 10^{-8} \cdot T^2 \end{array} \right. \\ \text{if } T < 143 \\ \quad \| k \leftarrow 0.014 \\ \text{if } T \ge 1050 \\ \quad \| k \leftarrow 0.069 \\ k \end{array} \right.$$

Convective heat transfer coefficient for cylinder wall (Woschni):

There are many heat transfer correlations. See summaries of Tuhovcak and of Disconzi. Correlations are sensitive to boundary and operating conditions. Calibration is required in many cases. Woschni gives results close to that of Disconzi (one of the newest (2006)) but is simpler to implement. Hence Woschni will be used.

Woschni	$Nu = 0.035\mathrm{Re}^{0.7}$	$\mathrm{Re} = \frac{u\,D}{\nu}$	$u = 6.618 \cdot u_p$ - opened valves $u = 2.28 \cdot u_p$ - closed valves

$CF_W := 18$

$$u(t, suc\_valve, dis\_valve) := \left| \begin{array}{l} \text{if } suc\_valve \vee dis\_valve = 1 \\ \quad \| 6.618 \cdot v_{shm}(t) \\ \text{else} \\ \quad \| 2.28 \cdot v_{shm}(t) \end{array} \right.$$

$$Re(T, t, suc\_valve, dis\_valve) := \frac{u(t, suc\_valve, dis\_valve) \cdot D_{cyl}}{\mu(T)}$$

$$hw(T, t, suc\_valve, dis\_valve) := 0.035 \cdot (Re(T, t, suc\_valve, dis\_valve))^{0.8} \cdot CF_W$$

$h_{wc}(t) := (s_{shm}(t) + h_{cle})$ Instantaneous cylinder wall height

$A_{cyl.wall}(t) := \pi \cdot D_{cyl} \cdot (s_{shm}(t) + h_{cle})$ Instantaneous circumferential wall area

$A_w(t) := ((A_{cyl} \cdot 2) + A_{cyl.wall}(t))$ Instantaneous total wall area

Differential equation function to be solved simultaneously with Runge-Kutta:

Energy:

$$dPdt(P, V, dVdt, m'_{in}, m'_{out}, T, \rho, t, h_w) := \frac{R \cdot \gamma}{V} \cdot (m'_{in} \cdot T_s - m'_{out} \cdot T) + \frac{R \cdot h_w \cdot A_w(t)}{C_v(T) \cdot V} \cdot (T_w - T) - dVdt \cdot \frac{P}{V} \cdot \left(\frac{R}{C_v(T)} + 1\right)$$

Mass:

$$dmdt(m'_{in}, m'_{out}) := (m'_{in}) - m'_{out}$$

Suction valve motion:

$$dydt(u) := u$$

$$dudt(y, u, P) := \frac{(C_{fs} \cdot A_s \cdot (P_s - P)) - k_s \cdot y}{m_{sv}}$$

Discharge valve motion:

$$dxdt(v) := v$$

$$dvdt(x, v, P) := \frac{(C_{fd} \cdot A_d \cdot (P - P_d)) - k_d \cdot x - F_{preload} - (c_{damping} \cdot v)}{m_{dv}}$$

Timed valve opening and closure:

$$Asv_{timed} := 2 \cdot \pi \cdot y_{timed} \cdot r_{sv}$$

$$Adv_{timed} := 2 \cdot \pi \cdot x_{timed} \cdot r_{dv}$$

$$\theta\_step\_size := \frac{2 \cdot \pi}{no\_divs}$$

$$d\theta := \theta\_step\_size$$

$$\theta_{so\_act} := \text{round}\left(\frac{\theta_{so}}{d\theta}\right) \cdot d\theta$$

$$\theta_{sc\_act} := \text{round}\left(\frac{\theta_{sc}}{d\theta}\right) \cdot d\theta$$

$$\theta_{do\_act} := \text{round}\left(\frac{\theta_{do}}{d\theta}\right) \cdot d\theta$$

$$\theta_{dc\_act} := \text{round}\left(\frac{\theta_{dc}}{d\theta}\right) \cdot d\theta$$

$$\theta_{so\_act.c} := \text{round}\left(\frac{\theta_{so.c}}{d\theta}\right) \cdot d\theta$$

$$\theta_{sc\_act.c} := \text{round}\left(\frac{\theta_{sc.c}}{d\theta}\right) \cdot d\theta$$

$$\theta_{do\_act.c} := \text{round}\left(\frac{\theta_{do.c}}{d\theta}\right) \cdot d\theta$$

$$\theta_{dc\_act.c} := \text{round}\left(\frac{\theta_{dc.c}}{d\theta}\right) \cdot d\theta$$

$$\theta_{cool\_act.s} := \text{round}\left(\frac{\theta_{s\_cool}}{d\theta}\right) \cdot d\theta$$

$$\theta_{cool\_act.e} := \text{round}\left(\frac{\theta_{e\_cool}}{d\theta}\right) \cdot d\theta$$

<u>Suction valve motion if timed:</u>
Valve displacement vs actuation cam angle was experimentally determined. A curve fit equation was derived with the following constants.

$c1 := 0.040917348$ $c2 := 0.203880272$ $c3 := 0.0643145771$ $c4 := 0.00505851277$

$c5 := 0.000103019891$

$$y_{s.rise}(\theta) := \frac{-c1 + c2 \cdot \left(\theta \cdot \frac{180}{\pi}\right) + c3 \cdot \left(\theta \cdot \frac{180}{\pi}\right)^2 - c4 \cdot \left(\theta \cdot \frac{180}{\pi}\right)^3 + c5 \cdot \left(\theta \cdot \frac{180}{\pi}\right)^4}{1000}$$

$c6 := 5.90382603$ $c7 := 0.0528239235$ $c8 := 0.01922864$ $c9 := 0.00278969369$

$c10 := 0.0000675602867$

$$y_{s.fall}(\theta) := \frac{c6 - c7\cdot\left(\theta\cdot\frac{180}{\pi}\right) + c8\cdot\left(\theta\cdot\frac{180}{\pi}\right)^2 - c9\cdot\left(\theta\cdot\frac{180}{\pi}\right)^3 + c10\cdot\left(\theta\cdot\frac{180}{\pi}\right)^4}{1000}$$

$y\_s(\theta) :=$

```
"Function: TIMED SUCTION VALVE MOTION"
"y_s = suction valve displacement at angle theta"
"Correct angles for curve fit equations:"
θcor.rise ← θ − θso.c
θcor.fall ← θ − (θsc.c − θfall)
"Suction valve rise period:"
if θ ≥ θso.c ∧ θ ≤ (θso.c + θrise)
    y_s ← ys.rise(θcor.rise)
"Suction valve fully open period:"
if θ > (θso.c + θrise) ∧ θ < (θsc.c − θfall)
    y_s ← y_max
"Suction valve fall period:"
if θ ≥ (θsc.c − θfall) ∧ θ ≤ θsc.c
    y_s ← ys.fall(θcor.fall)
y_s
```

Program variables:

$time\_one\_rev := \dfrac{1}{\dfrac{N}{60}}$ $\qquad time\_one\_rev = 0.1226743$

$Time\_step\_size := \dfrac{time\_one\_rev}{no\_divs}$ $\qquad Time\_step\_size = 0.000002453$

$\Delta t := Time\_step\_size$

$\dfrac{time\_one\_rev}{Time\_step\_size} = 50000$

$no\_of\_j\_loops := Number\_of\_revs$

Initial values:

$m'_{in_0} := 0$

$m'_{out_0} := 0$

$dVdt_0 := 0$

$P_0 := 0.9 \cdot P_d$

$T_0 := T_d$

$T_1 := T_0$

$\rho_0 := \dfrac{P_0}{R \cdot T_0}$

$h_{w_0} := 0.00000999$

$x_0 := 0.003$ $\quad$ $x_1 := 0.003$

$y_0 := y\_max$ $\quad$ $y_1 := y\_max$

$v_0 := 0$ $\quad$ $v_1 := 0$

$u_0 := 0$ $\quad$ $u_1 := 0$

$t_0 := 0$

$m_0 := \rho_0 \cdot V_{cle}$ $\quad$ $m_0 = 0.000050404$

$Wd_0 := 0$

$I_0 := 0$

$V_0 := V_{cle}$ $\quad$ $V_0 = 0.000014718$

$suc\_valve_0 := 0$ $\quad$ $dis\_valve_0 := 1$

$m_{cool_0} := m_{cool.cle}$ $\quad$ $m_{cool.cle} = 0$

$rho := \rho_0$

Write initial values to file:

$$init\_vals := \begin{bmatrix} x_0 & v_0 & t_0 & y_0 & u_0 & P_0 & V_0 & m'_{in_0} & m'_{out_0} & T_0 & \rho_0 & dVdt_0 & Wd_0 & I_0 & h_{w_0} & m_0 & m_{cool_0} \end{bmatrix}$$

Main Program:

```
M := | "ENERGY EQUATION"
     | "Time step:"
     | Δt ← Time_step_size
     | "Solution period (seconds):"
     | time_end ← time_one_rev · Number_of_revs
     | j ← 0
     | end ← time_end / Δt
     | for j ∈ 1 .. no_of_j_loops
     |   | "Read from file variables from end of previous rev. & declare new initial values for next rev."
     |   | ee ← READPRN(concat("aaC", num2str(j − 1), ".txt"))
     |   | x_0 ← ee_(0,0)
     |   | v_0 ← ee_(0,1)
     |   | t_0 ← ee_(0,2)
     |   | y_0 ← ee_(0,3)
     |   | u_0 ← ee_(0,4)
     |   | P_0 ← ee_(0,5)
     |   | V_0 ← ee_(0,6)
     |   | m'_in_0 ← ee_(0,7)
     |   | m'_out_0 ← ee_(0,8)
     |   | T_0 ← ee_(0,9)
     |   | ρ_0 ← ee_(0,10)
     |   | dVdt_0 ← ee_(0,11)
     |   | Wd_0 ← ee_(0,12)
     |   | I_0 ← ee_(0,13)
     |   | h_w_0 ← ee_(0,14)
     |   | m_0 ← ee_(0,15)
     |   | m_cool_0 ← ee_(0,16)
```

$$\theta_0 \leftarrow 0$$

$$\text{for } i \in 1 .. \frac{time\_one\_rev}{\Delta t}$$

$$t_i \leftarrow t_{i-1} + \Delta t$$

"Piston motion"

$$s_i \leftarrow s_{shm}(t_i)$$

$$V_i \leftarrow V_{cle} + s_i \cdot (A_{cyl})$$

"Angles:"

$$\theta_{rel_i} \leftarrow \begin{cases} \text{if } valves = 2 \vee 3 \vee 4 \\ \quad \theta_i \leftarrow \theta_{i-1} + d\theta \\ \quad tol_\theta \leftarrow d\theta \cdot 0.001 \\ \quad \theta_{rela_i} \leftarrow \left(\frac{\theta_i}{2 \cdot \pi} - \text{trunc}\left(\frac{\theta_i}{2 \cdot \pi}\right)\right) \cdot 2 \cdot \pi \\ \quad \theta_{rell_i} \leftarrow \begin{cases} \text{if } \theta_{rela_i} \geq tol_\theta \\ \quad \theta_{rela_i} \\ \text{else} \\ \quad 2 \cdot \pi \end{cases} \\ \text{else} \\ \quad 0 \end{cases}$$

"--"

"Runge-Kutta step 1"

$$k1\_P \leftarrow dPdt\left(P_{i-1}, V_{i-1}, dVdt_{i-1}, m'_{in_{i-1}}, m'_{out_{i-1}}, T_{i-1}, \rho_{i-1}, t_{i-1}, h_{w_{i-1}}\right)$$

$$k1\_v \leftarrow dvdt\left(x_{i-1}, v_{i-1}, P_{i-1}\right)$$

$$k1\_u \leftarrow dudt\left(y_{i-1}, u_{i-1}, P_{i-1}\right)$$

$$k1\_x \leftarrow dxdt\left(v_{i-1}\right)$$

$$k1\_y \leftarrow dydt\left(u_{i-1}\right)$$

$$k1\_m \leftarrow dmdt\left(m'_{in_{i-1}}, m'_{out_{i-1}}\right)$$

"--"

"Runge-Kutta step 2"

$$k2\_P \leftarrow dPdt\left(P_{i-1} + \frac{\Delta t}{2} \cdot k1\_P, V_{i-1}, dVdt_{i-1}, m'_{in_{i-1}}, m'_{out_{i-1}}, T_{i-1}, \rho_{i-1}, t_{i-1}, h_{w_{i-1}}\right)$$

$$k2\_v \leftarrow dvdt\left(\left(x_{i-1} + \frac{\Delta t}{2} \cdot k1\_x\right), \left(v_{i-1} + \frac{\Delta t}{2} \cdot k1\_v\right), \left(P_{i-1} + \frac{\Delta t}{2} \cdot k1\_P\right)\right)$$

$$k2\_u \leftarrow dudt\left(\left(y_{i-1} + \frac{\Delta t}{2} \cdot k1\_y\right), \left(u_{i-1} + \frac{\Delta t}{2} \cdot k1\_u\right), \left(P_{i-1} + \frac{\Delta t}{2} \cdot k1\_P\right)\right)$$

$$k2\_x \leftarrow dxdt\left(v_{i-1} + \frac{\Delta t}{2} \cdot k1\_x\right)$$

$k2\_y \leftarrow dydt\left(u_{l-1} + \frac{\Delta t}{2} \cdot k1\_y\right)$

$k2\_m \leftarrow dmdt\left(\left(m'_{in_{l-1}} + \frac{\Delta t}{2} \cdot k1\_m\right), \left(m'_{out_{l-1}} + \frac{\Delta t}{2} \cdot k1\_m\right)\right)$

"____________________________________"

"Runge-Kutta step 3"

$k3\_P \leftarrow dPdt\left(P_{l-1} + \frac{\Delta t}{2} \cdot k2\_P, V_{l-1}, dVdt_{l-1}, m'_{in_{l-1}}, m'_{out_{l-1}}, T_{l-1}, \rho_{l-1}, t_{l-1}, h_{w_{l-1}}\right)$

$k3\_v \leftarrow dvdt\left(\left(x_{l-1} + \frac{\Delta t}{2} \cdot k2\_x\right), \left(v_{l-1} + \frac{\Delta t}{2} \cdot k2\_v\right), \left(P_{l-1} + \frac{\Delta t}{2} \cdot k2\_P\right)\right)$

$k3\_u \leftarrow dudt\left(\left(y_{l-1} + \frac{\Delta t}{2} \cdot k2\_y\right), \left(u_{l-1} + \frac{\Delta t}{2} \cdot k2\_u\right), \left(P_{l-1} + \frac{\Delta t}{2} \cdot k2\_P\right)\right)$

$k3\_x \leftarrow dxdt\left(v_{l-1} + \frac{\Delta t}{2} \cdot k2\_x\right)$

$k3\_y \leftarrow dydt\left(u_{l-1} + \frac{\Delta t}{2} \cdot k2\_y\right)$

$k3\_m \leftarrow dmdt\left(\left(m'_{in_{l-1}} + \frac{\Delta t}{2} \cdot k2\_m\right), \left(m'_{out_{l-1}} + \frac{\Delta t}{2} \cdot k2\_m\right)\right)$

"____________________________________"

"Runge-Kutta step 4"

$k4\_P \leftarrow dPdt\left(P_{l-1} + \Delta t \cdot k3\_P, V_{l-1}, dVdt_{l-1}, m'_{in_{l-1}}, m'_{out_{l-1}}, T_{l-1}, \rho_{l-1}, t_{l-1}, h_{w_{l-1}}\right)$

$k4\_v \leftarrow dvdt\left(\left(x_{l-1} + \Delta t \cdot k3\_x\right), \left(v_{l-1} + \Delta t \cdot k3\_v\right), \left(P_{l-1} + \Delta t \cdot k3\_P\right)\right)$

$k4\_u \leftarrow dudt\left(\left(y_{l-1} + \Delta t \cdot k3\_y\right), \left(u_{l-1} + \Delta t \cdot k3\_u\right), \left(P_{l-1} + \Delta t \cdot k3\_P\right)\right)$

$k4\_x \leftarrow dxdt\left(v_{l-1} + \Delta t \cdot k3\_x\right)$

$k4\_y \leftarrow dydt\left(u_{l-1} + \Delta t \cdot k3\_y\right)$

$k4\_m \leftarrow dmdt\left(\left(m'_{in_{l-1}} + \Delta t \cdot k3\_m\right), \left(m'_{out_{l-1}} + \Delta t \cdot k3\_m\right)\right)$

"____________________________________"

"Runge-Kutta final step"

$P_l \leftarrow P_{l-1} + \frac{\Delta t}{6} \cdot (k1\_P + 2 \cdot k2\_P + 2 \cdot k3\_P + k4\_P)$

"____________________________________"

"Valve motion:"

"Discharge valve:"

$x_l \leftarrow$ if $valves = 0 \vee 4$

if $0 \le x_{l-1} \le x\_max$

$x_{l-1} + \frac{\Delta t}{6} \cdot (k1\_x + 2 \cdot k2\_x + 2 \cdot k3\_x + k4\_x)$

if $x_{l-1} < 0$

0

if $x_{l-1} > x\_max$

x_max

else
-99
if $valves = 1$
if $P_i > P_d$
x_max
else
0
if $valves = 2$
if $\theta_{do\_act} \le \theta_{rel_{i-1}} \le \theta_{dc\_act}$
x_{timed}
else
0
if $valves = 3$
if $\theta_{do\_act.c} \le \theta_{rel_{i-1}} \le \theta_{dc\_act.c}$
x_{timed}
else
0
"Suction valve:"
$y_i \leftarrow$ if $valves = 0$
if $0 \le y_{i-1} \le y\_max$
$$y_{i-1} + \frac{\Delta t}{6} \cdot (k1\_y + 2 \cdot k2\_y + 2 \cdot k3\_y + k4\_y)$$
if $y_{i-1} < 0$
0
if $y_{i-1} > y\_max$
y_max
else
-99
if $valves = 1$
if $P_s > P_i$
y_max
else
0
if $valves = 2$
if $\theta_{so\_act} \le \theta_{rel_{i-1}} \le \theta_{sc\_act}$
y_{timed}

else

0

if $valves = 3$

if $\theta_{so\_act.c} \le \theta_{rel_{i-1}} \le \theta_{sc\_act.c}$

y_{timed}

else

0

if $valves = 4$

if $\theta_{so\_act.c} \le \theta_{rel_{i-1}} \le \theta_{sc\_act.c}$

$y\_s\left(\theta_{rel_i}\right)$

else

0

"VALVE VELOCITIES"

$v_i \leftarrow$ if $0 \le x_{i-1} \le x\_max$

$v_{i-1} + \frac{\Delta t}{6} \cdot (k1\_v + 2 \cdot k2\_v + 2 \cdot k3\_v + k4\_v)$

else

0

$u_i \leftarrow$ if $0 \le y_{i-1} \le y\_max$

$u_{i-1} + \frac{\Delta t}{6} \cdot (k1\_u + 2 \cdot k2\_u + 2 \cdot k3\_u + k4\_u)$

else

0

"VALVE POSITION CHECKS"

"Is suction valve open? "

$suc\_valve \leftarrow$ "(0 = close; 1 = open)"

if $valves = 0$

if $y_i > 0$

1

else

0

if $valves = 1$

if $y_i > 0$

1

else

0

""

if $valves = 2$

if $\theta_{so\_act} \le \theta_{rel_{i-1}} \le \theta_{sc\_act}$

1

else

0

if $valves = 3$

if $\theta_{so\_act.c} \le \theta_{rel_{i-1}} \le \theta_{sc\_act.c}$

1

else

0

if $valves = 4$

if $\theta_{so\_act.c} \le \theta_{rel_{i-1}} \le \theta_{sc\_act.c}$

1

else

0

"Is discharge valve open? "

$dis\_valve \leftarrow$ if $valves = 0 \vee 1$

if $x_i > 0$

1

else

0

if $valves = 2$

if $\theta_{do\_act} \le \theta_{rel_{i-1}} \le \theta_{dc\_act}$

1

else

0

if $valves = 3$

if $\theta_{do\_act.c} \le \theta_{rel_{i-1}} \le \theta_{dc\_act.c}$

1

else

0

if $valves = 4$

if $x_i > 0$

1

else

0

"Is coolant injected? "

""

$cool\_inj \leftarrow$ if $valves = 3$

if $\theta_{cool\_act.s} \le \theta_{rel_{i-1}} \le \theta_{cool\_act.e}$

1

else

0

if $valves = 4$

if $\theta_{cool\_act.s} \le \theta_{rel_{i-1}} \le \theta_{cool\_act.e}$

1

else

0

"--"

$$dVdt_i \leftarrow \frac{V_i - V_{i-1}}{\Delta t}$$

$$m_i \leftarrow m_{i-1} + \frac{\Delta t}{6} \cdot (k1\_m + 2 \cdot k2\_m + 2 \cdot k3\_m + k4\_m)$$

$$\rho_i \leftarrow \frac{m_i}{V_i}$$

"--"

"MASS FLOW RATES"

"(m`.in and m`.out are mass flow rates in kg/s)"

"The pressure at time i is used to calculate the mass at time i"

"Suction valve timing"

$m'_{in_i} \leftarrow$ if $suc\_valve = 1 \wedge (P_s > P_i)$

$$Cd(y_i, D_{sv}) \cdot \rho_s \cdot (\pi \cdot y_{i-1} \cdot D_{sv}) \cdot \sqrt{\frac{2 \cdot (P_s - P_i)}{\rho_s}}$$

else if $suc\_valve = 1 \wedge (P_i > P_s)$

$$-\left(Cd(y_i, D_{sv}) \cdot \rho_s \cdot (\pi \cdot y_{i-1} \cdot D_{sv}) \cdot \sqrt{\frac{2 \cdot (P_i - P_s)}{\rho_i}}\right)$$

else

0

"--"

"Discharge valve timing"

$m'_{out_i} \leftarrow$ if $dis\_valve = 1 \wedge (P_i > P_d)$

$$Cd(x_i, D_{dv}) \cdot \rho_i \cdot (\pi \cdot x_{i-1} \cdot D_{dv}) \cdot \sqrt{\frac{2 \cdot (P_i - P_d)}{\rho_i}}$$

else if $dis\_valve = 1 \wedge (P_d > P_i)$

$$-\left(Cd\left(x_i, D_{dv}\right) \cdot \rho_i \cdot \left(\pi \cdot x_{i-1} \cdot D_{dv}\right) \cdot \sqrt{\frac{2 \cdot \left(P_d - P_i\right)}{\rho_d}}\right)$$

else

0

"--"

"Coolant mass flow rate out"

$m'_{cool.out_i} \leftarrow m'_{coolant\_frac} \cdot m'_{out_i}$

"--"

"Coolant mass in cylinder"

$m_{cool_i} \leftarrow$ "--- During expansion:"

if $suc\_valve = 0 \wedge \left(V_i > V_{i-1}\right)$

$m_{cool_{i-1}}$

else if $suc\_valve = 1 \wedge \left(V_i > V_{i-1}\right)$

"--- During suction:"

$m_{cool_{i-1}}$

else if $valves = 4 \wedge \theta_{so\_act.c} \leq \theta_{rel_{i-1}} \leq \theta_{sc\_act.c}$

"--- During coolant injection:"

$m_{cool_{i-1}} + m'_{cool} \cdot \Delta t$

else if $valves = 4 \wedge \theta_{sc\_act.c} < \theta_{rel_i} \wedge dis\_valve = 0$

"--- During compression after coolant injection stopped:"

$m_{cool_{i-1}}$

else if $dis\_valve = 1 \wedge valves = 3 \wedge valves = 4$

"--- During discharge:"

$m_{cool_{i-1}} - m'_{cool.out_i} \cdot \frac{\Delta t}{3.44}$

else

$m_{cool_{i-1}}$

"--"

"Cylinder temperature without infuence of any in flows"

$T_i \leftarrow$ if $valves = 0 \vee 1 \vee 2$

if $suc\_valve = 1$

$$\frac{\left(m_{i-1} \cdot T_{i-1}\right) + \left(\left(m'_{in_i} \cdot \Delta t\right) \cdot T_s\right)}{\left(m_{i-1} + \left(m'_{in_i} \cdot \Delta t\right)\right)}$$

else

$$\frac{P_i}{R \cdot \rho_i}$$

if $valves = 4$

if $suc\_valve = 1$

$$\frac{\left(m_{l-1} \cdot T_{l-1}\right) + \left(\left(m'_{in_l} \cdot \Delta t\right) \cdot T_s\right)}{\left(m_{l-1} + \left(m'_{in_l} \cdot \Delta t\right)\right)}$$

if $cool\_inj = 1$

$$\frac{\left(m_{l-1} \cdot T_{l-1}\right) + \left(\left(m'_{cool} \cdot \Delta t\right) \cdot T_{cool}\right)}{\left(m_{l-1} + \left(m'_{cool} \cdot \Delta t\right)\right)}$$

else

$$\frac{P_l}{R \cdot \rho_l}$$

$P_l \leftarrow T_l \cdot R \cdot \rho_l$

$\rho_l \leftarrow \dfrac{P_l}{R \cdot T_l}$

"___________________________________"

$h_{w_l} \leftarrow hw\left(T_l, t_l, suc\_valve, dis\_valve\right)$

"___________________________________"

"Instantanuous work done:"

$Wd_l \leftarrow \left(P_l - P_{l-1}\right) \cdot \dfrac{\left(V_l + V_{l-1}\right)}{2}$

"___________________________________"

$I_l \leftarrow i$

"Total work done per cycle:"

$W \leftarrow \sum Wd$

WRITEPRN(concat("WorkC4T", ".txt"), W)

WRITEPRN(("T_Dis.txt"), T)

"CONVERGENCE CHECK PARAMETERS"

"Calculate differences between means of variables for j and j-1 loops:"

$m_{mean_j} \leftarrow \text{mean}\left(m_j\right)$

$P_{mean_j} \leftarrow \text{mean}\left(P_j\right)$

$T_{mean_j} \leftarrow \text{mean}\left(T_j\right)$

$dm\_dt_j \leftarrow m_{mean_j} - m_{mean_{j-1}}$

$dPmdt_j \leftarrow P_{mean_j} - P_{mean_{j-1}}$

$dTmdt_j \leftarrow T_{mean_j} - T_{mean_{j-1}}$

$x\_mean_j \leftarrow \text{mean}\left(x_j\right)$

$dXdt_j \leftarrow x\_mean_j - x\_mean_{j-1}$

$y\_mean_j \leftarrow \text{mean}\left(y_j\right)$

$dYdt_j \leftarrow y\_mean_j - y\_mean_{j-1}$

$\rho_{mean_j} \leftarrow \text{mean}\left(\rho_j\right)$

$d\rho mdt_j \leftarrow \rho_{mean_j} - \rho_{mean_{j-1}}$

"Write differences between means of variables to file:"
WRITEPRN(concat("1dmdtC4T", ".txt"), dm_dt)
WRITEPRN(concat("2dPdtC4T", ".txt"), dPmdt)
WRITEPRN(concat("3dTdtC4T", ".txt"), dTmdt)
WRITEPRN(concat("4dXdtC4T", ".txt"), dXdt)
WRITEPRN(concat("5dYdtC4T", ".txt"), dYdt)
WRITEPRN(concat("6dDenC4T", ".txt"), dρmdt)
"————————————————————"

"Write to file variables at end of i loop j times"

$vars\_i\_j \leftarrow \text{augment}\left(x_j, v_j, t_j, y_j, u_j, P_j, V_j, m'_{in_j}, m'_{out_j}, T_j, \rho_j, dVdt_j, Wd_j, I_j, h_{w_j}, m_j, m_{cool_j}\right)$

$vars\_i\_j\_prev \leftarrow \text{READPRN}(\text{concat}(\text{"aaC"}, \text{num2str}(j-1), \text{".txt"}))$

$\text{WRITEPRN}(\text{concat}(\text{"aaC"}, \text{num2str}(j), \text{".txt"}), vars\_i\_j)$

$Result \leftarrow \text{augment}(x, v, t, y, u, P, V, m'_{in}, m'_{out}, T, \rho, dVdt, Wd, m, h_w, m_{cool})$

"Stop loop j with "break" statement if tolerance for variances (residuals) is satisfied:"

$x_{i\_j\_prev} \leftarrow vars\_i\_j\_prev_{0,0}$

$P_{i\_j\_prev} \leftarrow vars\_i\_j\_prev_{0,5}$

$T_{i\_j\_prev} \leftarrow vars\_i\_j\_prev_{0,9}$

$$break\_x \leftarrow \left\| \begin{array}{l} \text{if } \dfrac{\left|x_j - x_{i\_j\_prev}\right|}{x_j + 0.00001} \le tol_x \\ \quad \| 1 \\ \text{else} \\ \quad \| 0 \end{array} \right.$$

$$break\_P \leftarrow \left\| \begin{array}{l} \text{if } \left|P_j - P_{i\_j\_prev}\right| \le tol_P \\ \quad \| 1 \\ \text{else} \\ \quad \| 0 \end{array} \right.$$

$$break\_T \leftarrow \left\| \begin{array}{l} \text{if } \left|T_j - T_{i\_j\_prev}\right| \le tol_T \\ \quad \| 1 \\ \text{else} \\ \quad \| 0 \end{array} \right.$$

$$break\_m \leftarrow \left\| \begin{array}{l} \text{if } \dfrac{\left|dm\_dt_j\right|}{\sum m'_{in}} \le tol_m \end{array} \right.$$

```
            1
        else
            0
    if (break_x = 1) ∧ (break_P = 1) ∧ (break_T = 1) ∧ (break_m = 1) ∧ (j > 4)
        break
WRITEPRN("j.txt", j)
Result
```